POLYMETALLIC LUMINESCENT DENDRIMER-LANTHANIDE COMPLEXES

by

Grzegorz Pawel. Filipczyk

Chemistry, MS, University of Silesia, 1992

Submitted to the Graduate Faculty of

Arts and Sciences in partial fulfillment

of the requirements for the degree of

Master of Science

University of Pittsburgh

2006

UNIVERSITY OF PITTSBURGH

FACULTY OF ARTS AND SCIENCES

This dissertation was presented

by

Grzegorz Pawel Filipczyk

It was defended on

December 13, 2005

and approved by

Dr. Toby Chapman

Dr. Bodie Douglas

Dr. Stéphane Petoud
Dissertation Director

POLYMETALLIC LUMINESCENT DENDRIMER-LANTHANIDE COMPLEXES

Grzegorz Pawel Filipczyk, MS

University of Pittsburgh, 2006

The medical and biological fields of today have high demands for luminescent molecules for fluorescence microscopy and imagery that can report biological activities or would allow the quantification of in vivo biologically relevant molecules or ions. Fluorescence microscopy is a principal technique due to its high sensitivity and versatility.

This work explores a new concept to optimize the intensity of luminescent complexes by maximizing the number of lanthanide cations and the number of sensitizing groups per discrete molecule of complex. PAMAM (polyamidoamine) dendrimer ligands have been chosen as the coordinating unit for the formation of these polymetallic lanthanide complexes. Generation 3 dendrimer possess 60 amide groups, i.e. 60 oxygen groups to bind 7-8 lanthanide cations with a coordination number of 9. In addition, the globular structure of the dendrimer is expected to shield the lanthanide cations from molecules (such as water) that can diminish the luminescence of the complex through non-radiative deactivation. Another advantage of this strategy is that sensitizers do not need to be directly bound to the metal ion, allowing for a broader choice of lanthanide sensitizers. A family of naphthalimide groups was chosen as sensitizers because of the high population of their triplet state, a desirable property for the ligand to lanthanide energy transfer, and their sensitivity to oxygen molecules. Preliminary experiments have demonstrated that each of the dendrimer-naphthalimide ligand is able to coordinate eight Ln^{3+} cations. These ligands are able to sensitize several visible and NIR emitting lanthanides.

The luminescent neodymium complexes were injected into the cells and the emission intensity was monitored through near-infrared fluorescence microscopy. The fluorescence intensity was proportional to the concentration of oxygen present in the cell. The decrease of oxygen concentration from 21% to 1.5% induced an increase of the luminescence signal of 60%. These preliminary experiments are the first examples of a luminescent lanthanide complex emitting in the near-infrared domain used for fluorescence microscopy. It demonstrates that the complex used is luminescent and stable enough to be used as a reporter in physiological conditions.

TABLE OF CONTENTS

LIST OF TABLES

LIST OF FIGURES

ABBREVIATIONS

°C	Celcius
C	Concentration
cps	Counts per second
DAF	Delay After Flash
DMSO	Dimethyl sulfoxide
e.g.	Exempli gratia (for example)
eq	Equivalents
ET	Energy transfer
h	Planck constant
HOMO	Highest occupied molecular orbital
IC	Internal Conversion
ISC	Intersystem crossing
K	Kelvin
Ln	Lanthanide
LUMO	Lowest unoccupied molecular orbital
mg	Milligram
ml	Milliliter
mm	Millimeter
MRI	Magnetic resonance imaging
ms	Millisecond
nm	Nanometer
NF	Number of Flashes
NMR	Nuclear magnetic resonance
No	Number

PAMAM	Polyamidoamine
QY	Quantum Yield
rt	Room temperature
SW	Sample Window (Gate Time)
s	Second
S_0	Electronic ground state
S_1	First excited electronic state
TPF	Time Per Flash
T	Triplet state
μl	Microliter
μs	Microsecond
ν	Frequency

ACKNOWLEDGMENTS

1.0   INTRODUCTION

1.1 LUMINESCENT LANTHANIDE COMPLEXES

The Laporte selection rule states that transitions involving the redistribution of electrons in one quantum shell are parity forbidden.[1,2] This includes p → p, d → d and, important for lanthanides, f → f transitions. There are some factors, however, such as interactions with the ligand field or mixing of electronic states with vibrational states that make these transitions more allowed. Nevertheless, the probability of such transitions is low; for f → f transitions the molar absorption coefficients (ε) are in the order of 1 or less.

It is possible to increase a lanthanide ion's emission by placing it at close proximity to an antenna.[1] In this approach, molecules such as organic chromophores are attached to the lanthanide. The chromophore acts as sensitizer by absorbing light of appropriate wavelength, and converting the resulting energy to the lanthanide ion. This process is schematically depicted in Figure 1-1:
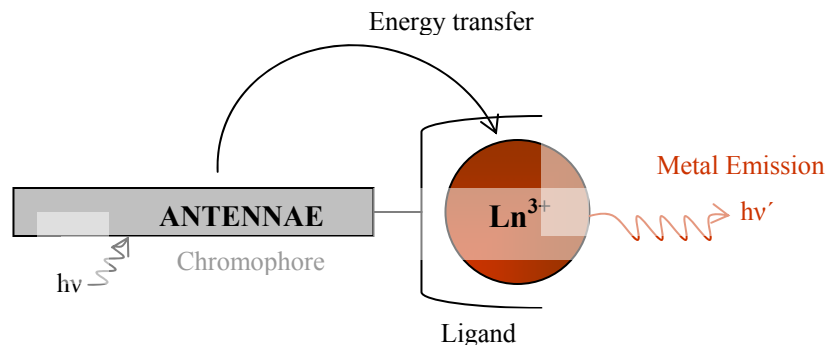
Figure 1-1: The antenna effect: Schematic representation

After absorption of the light by the organic chromophore an electron is promoted to the excited energy level. There are several competitive ways for deactivation of the absorbed energy and relaxation of the electron to the ground state (S_0). This occurs by intrinsic first order kinetic processes[3] depicted schematically in Figure 1-2.

Deactivation can happen in form of *fluorescence*,[4] where non-radiative relaxation occurs to the lowest vibrational level in the excited electronic state (S_1), followed by a radiative decay to the electronic ground state (S_0) at the rate constant k^F. Fluorescence lifetimes are in the order of 10^{-12} – 10^{-9} s. Competitively, the excited state can undergo deactivation via non-radiative relaxation to the ground state (*internal conversion*, IC) at the rate constant k_{nr}^F.

The third route for the excited chromophore to relax to the ground state (S_0) is *phosphorescence*[4] with lifetimes between 10^{-6} s. and seconds. At a certain vibrational level the molecule undergoes intersystem crossing (ISC) from a singlet (S_1) to a triplet state (T_1) at the rate constant k_{iSC}, reach the lowest vibrational level of the triplet state through non-radiative relaxation, and then returns to the ground state (S_0) by a spin-forbidden transition at the rate constant k^P. This spin-forbidden transition is responsible for the low kinetic rate constant of phosphorescence and long

luminescence lifetimes (milliseconds to seconds).[3] Again, non-radiative deactivation (IC) competes with the phosphorescence (at the rate constant k_{nr}^P).

Another possibility is energy transfer to the metal ion, a process called *external conversion* (EC), which is a non-radiative transition to a low lying accepting level of the lanthanide ion (rate constant k_{et}). Due to this transition one of the lanthanide´s electrons is promoted to an excited 4f-level and can then relax to the ground state (at the rate constant k_{Ln}) with the emission of a photon specific to the lanthanide ion. This process also competes with non-radiative vibrational deactivation ($k_{nr}^{vibr(T)}$) and with back energy transfer to the triplet state (k_{back}) if the energy difference between triplet state and accepting level of lanthanide is small enough.
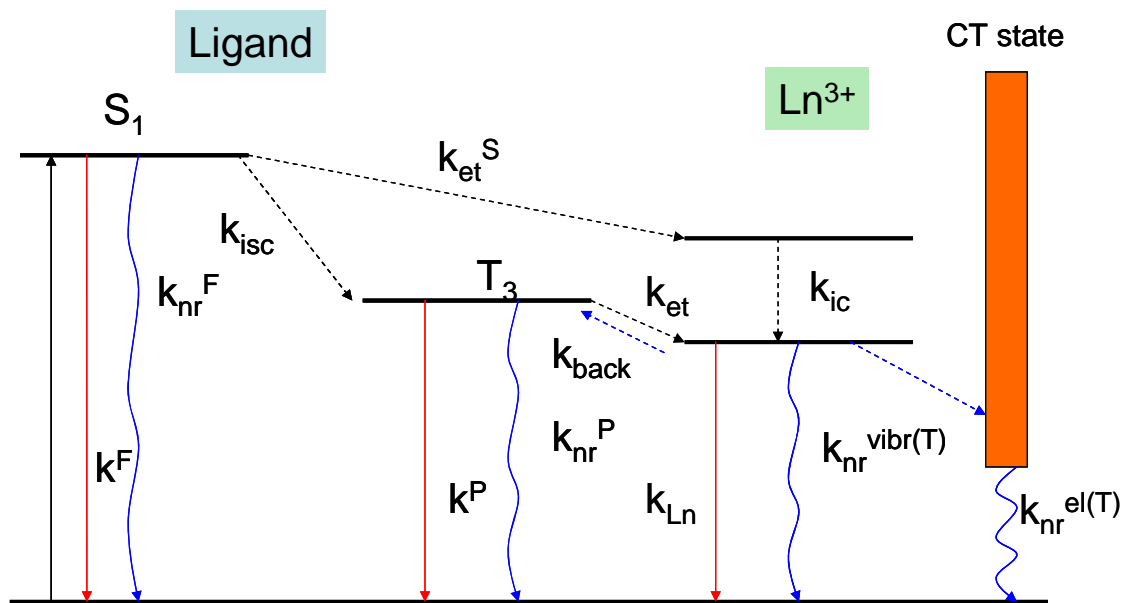
Figure 1-2: Diagram illustrating various deactivation processes of the excited state and the antenna effect.

In theory, energy transfer from the excited state (S_1) to the Ln^{3+} ion is also possible (at the rate constant k_{et}^S), but it is believed that the luminescence lifetimes of the singlet excited states are too short to play a major role in the energy transfer.

Another possible deactivation process is electron transfer to an accepting energy level of a neighbouring species, called the charge transfer process (CT). Exactly speaking this is an electron transfer process leading to changes in the oxidation states of the interacting molecules.[3] Energy conversion to the CT energy level is followed by non-radiative deactivation to the ground state at the rate constant $k_{nr}^{el(T)}$.

Finally, the excited species can undergo photochemical reaction such as rupture of the bond, isomerisation or fragmentation of the species.

Energy and electron transfer processes can occur between distinct molecules as well as between molecular components of the multi-component species like dendrimer complexes. Energy and electron transfer processes between components of such systems take place with first order kinetics.

The kinetic constants of the various deactivation processes usually can not be measured directly; however luminescence *lifetimes* (τ) which are the reciprocals of the first order deactivation rate constants can be measured directly.[3]

The *quantum yield* (QY) reflects the efficiency of the energy transfer and non-radiative deactivation. QY is defined as the ratio of the number of emitted photons to the number of absorbed photons.

Since the measurement of absolute quantum yields is technically challenging and time consuming, relative quantum yields are often measured instead. Here the quantum yield of an unknown sample is measured relative to a compound with a well known quantum yield values. The quantum yields of the standard and the sample are related by the following equation 1-1:[5]

$$\Phi_{(S)} = \left(\frac{A_{(R)}}{A_{(S)}}\right)\left(\frac{I_{(S)}}{I_{(R)}}\right)\left(\frac{F_{(S)}}{F_{(R)}}\right)\left(\frac{\eta_{(S)}}{\eta_{(R)}}\right)^2 \Phi_{(R)} \tag{1-1}$$

A is the absorbance at the excitation wavelength, I is the intensity of the excitation light at the same wavelength, F is the area under the corrected emission curve and η is the refractive index of the solvents used. The subscripts S and R refer to sample and reference respectively.

Excited states of lanthanide cations can be deactivated through O-H, N-H, C-H vibrations.[1, 2, 6] The efficiency of this quenching process depends partially on the energy gap between the ground and excited states and the vibrational energy of the oscillators.[1] Figure 1-3 shows selected oscillators and their energies in relation to selected lanthanides.
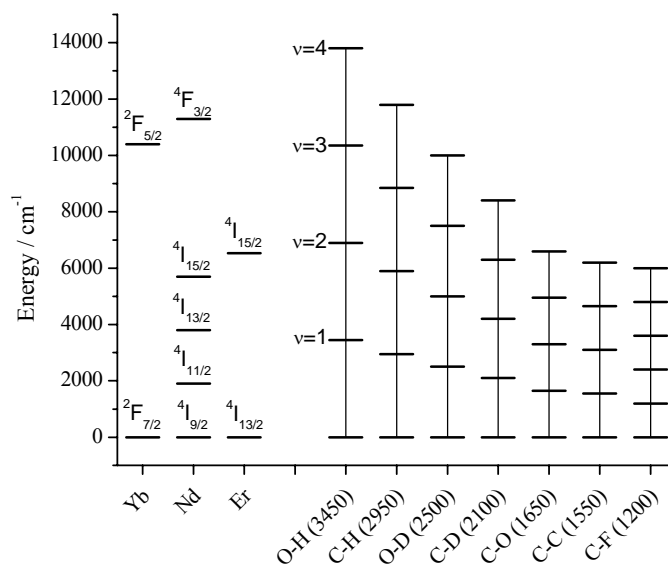
Figure 1-3: Non-radiative deactivation through vibrational energies of selected quenchers[7].

5

The most effective quencher is the high energy O-H oscillator; therefore care must be applied in designing ligands that contain minimal amount of quenching oscillators and protect lanthanide ions from solvent molecules such as H_2O. The number of water molecules around the lanthanide ion coordinated to the ligand can be calculated from the Parker's equation (1-2).[6, 8]

$$q' = A'_{Ln} [(k_{H_2O} - k_{D_2O}) + corr_{Ln}] \qquad (1\text{-}2)$$

where q' is the inner sphere hydration number, A'_{Ln} is an empirical tabulated value, k is the rate constant for depopulation of the lanthanide excited state in H_2O and D_2O respectively, $corr_{Ln}$ is the correction for the water molecules in the outer coordination sphere.

There are three main mechanisms for the energy transfer from the chromophore to the ligand described in the literature: *Förster*, Dexter, and *electron transfer* mechanisms (depicted in Figure 1-4, Figure 1-5 and Figure 1-6.[1, 9]
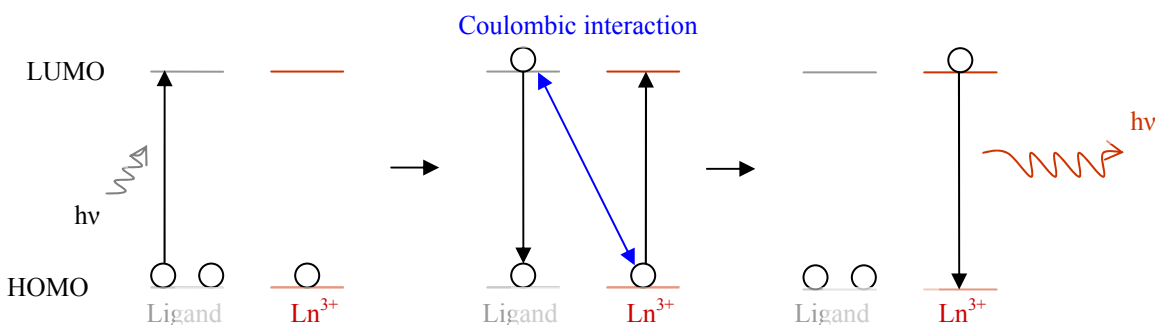
Figure 1-4: *Förster* mechanism of the energy transfer.[7]
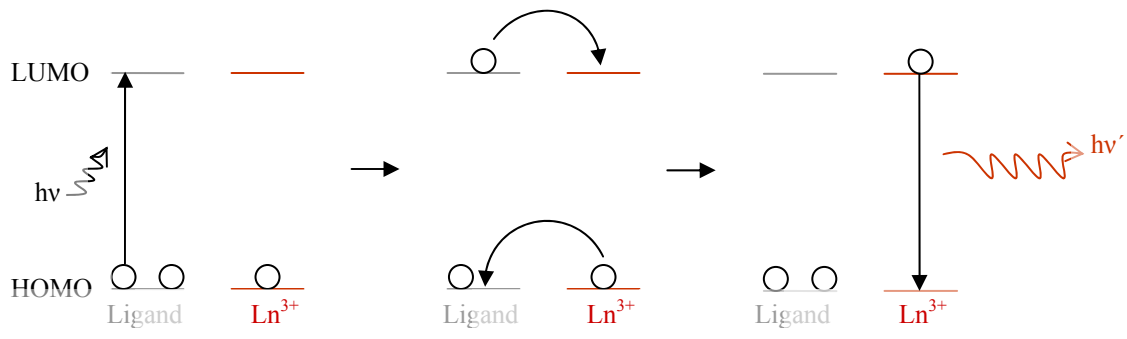
Figure 1-5: *Dexter* **mechanism of the energy transfer.**[7]
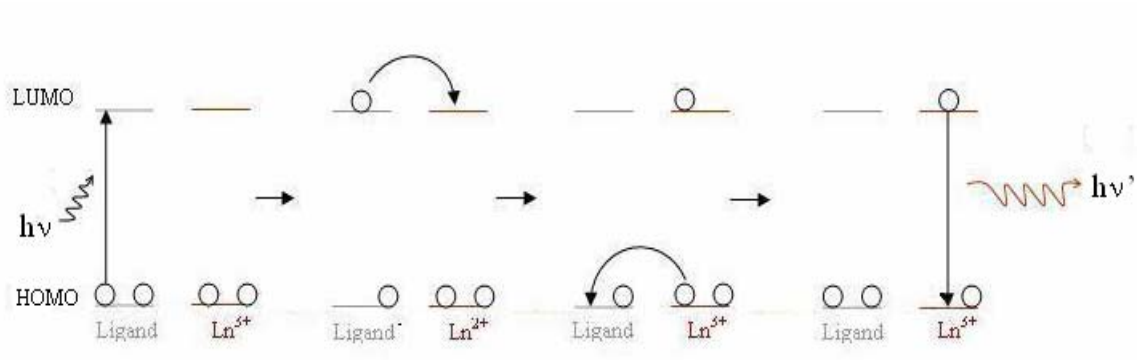
Figure 1-6: Electron transfer mechanism.

The *Förster* mechanism is a purely coulombic interaction which does not require orbital overlap. After exciting the ligand which acts as an antenna, the excited electron can return to the electronic ground state. In this process energy is transferred to the lanthanide ion by inducing a dipole oscillation in the acceptor (in this case the Ln^{3+} Ion) and as a consequence one of the metal ion´s 4f-electrons is promoted to the excited electronic state (S_1). This electron can then be relaxed to the ground state (S_0), emitting a photon specific to the lanthanide ion´s electronic structure.

In contrast to the *Förster* mechanism the *Dexter* mechanism does require orbital overlap, since it involves simultaneous electron exchange from the antenna to the lanthanide ion and vice versa. The ligand´s excited electron is transferred to the metal ion´s excited electronic state and at the same time one of the electrons in the lanthanide ion´s ground state is transferred to the ligand. The electron in the Ln^{3+} excited state can then relax to the ground state, emitting a photon specific to the lanthanide ion.

The third mechanism of the energy transfer is the *electron transfer* mechanism. The lanthanides ions that have red-ox potential low enough such as Eu^{3+}, Sm^{3+} and Yb^{3+} can act as electron acceptor. The ligand acts as an electron donor. After absorption of light by the ligand, an electron is transferred from the ligand excited energy level to the lanthanide excited energy level which causes reduction of the lanthanide ion and oxidation of the ligand. In the next step, an electron from the ground energy level of the lanthanide ion returns to the ground energy level of the ligand. In result both ligand and lanthanide return to their original oxidation states. In the last step the electron from the excited state of the lanthanide ion relaxes to the ground state emitting photon.

The energy levels of several lanthanide ions are depicted in Figure 1-7. There are four lanthanide ions that emit in the visible (samarium, europium, terbium and dysprosium) and six that emit in the near infrared (praseodymium, neodymium, holmium, erbium, thulium and ytterbium).
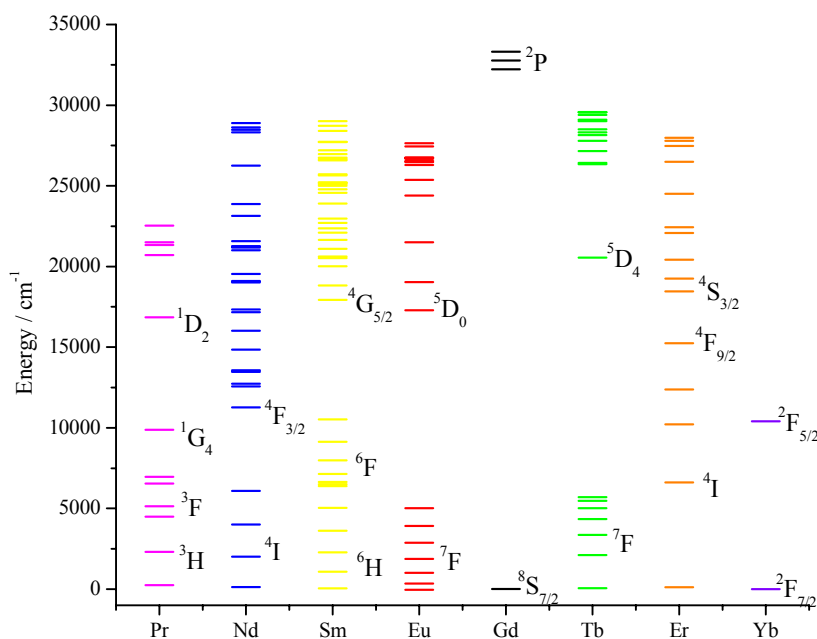
Figure 1-7: Selected electronic levels of several luminescent lanthanide cations.[7]

1.2 LUMINESCENT LANTHANIDES VS ORGANIC FLUOROPHORES - APPLICATIONS OF THE LANTHANIDE COMPLEXES

Applications for lanthanide-complexes have been developed based on their unique electronic properties, which were partly described above. They can be divided in two groups, namely the applications utilizing luminescence properties and those based on the magnetic properties of lanthanide ions. We will focus on the luminescence properties.

Lanthanide complexes have several advantages over organic fluorophores for bioanalytical applications. Lanthanide complexes usually do not photobleach. Illustrated in Figure 1-8, the luminescence intensity of a lanthanide complex prepared in our group remains constant with

9

time, while the emission of a well known organic fluorophore, indocyanine green, decreases significantly with time (only 30% of residual fluorescence after 55 minutes). The electron-deficient lanthanide cation stabilizes the excited states of bound organic ligands, preventing irreversible photo-reactions when the complex is irradiated. This yields a long shelf life, easy manipulation of these luminescent probes, and most importantly, allowance for long exposure times and repeated experiments.
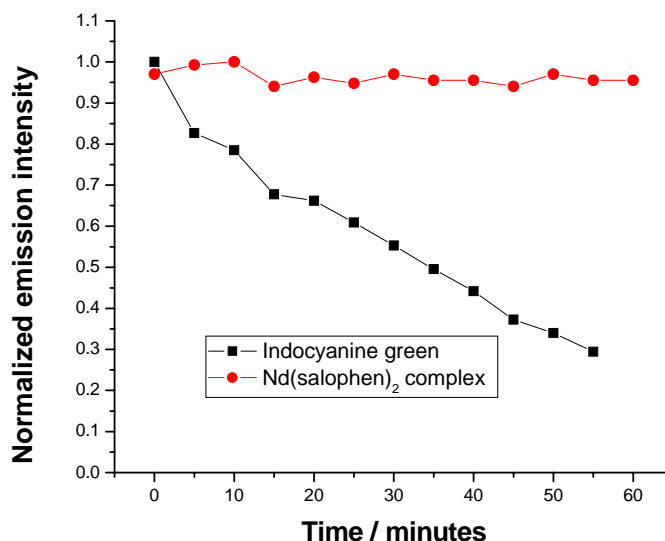
Figure 1-8: Relative emission intensities versus time for a luminescent Neodymium complex Na[Nd(salophen)$_2$] developed in our group (6.5x10-6M in DMSO) and indocyanine green (1.3x10-6M in DMSO).[7]

Luminescent lanthanide cations (free and in complexes) also have sharp, atomic-like emission bands (Figure 1-9). The energy positions of these bands do not vary with changes of experimental conditions such as temperature, pressure or pH. The bandwidths are significantly narrower than those of organic fluorophores and have only minimal overlap. This property allows detecting several lanthanide emissions independently during the same experiment, a

10

desirable advantage for multiplex analysis. Drug discovery processes, for example, could be completed faster by carrying out several assays simultaneously. There is a large energy gap between the absorption and emission bands of lanthanide complexes. This unique property allows lanthanide emission bands to be easily spectrally discriminated from other signals.
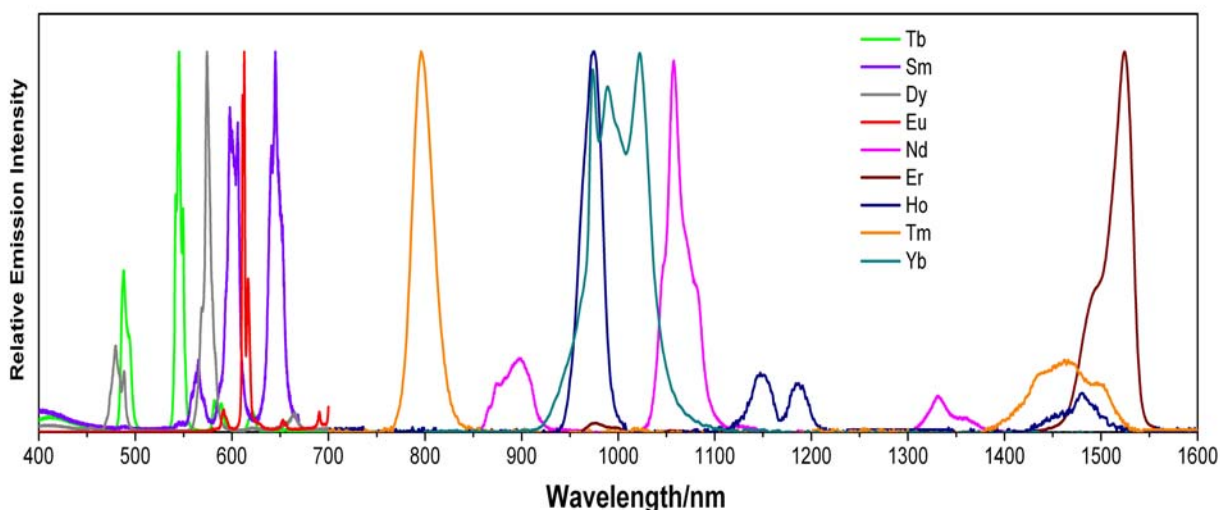
Figure 1-9: Emission spectra of the lanthanides that emit in the visible and NIR.[10, 11]

The luminescence lifetimes of lanthanide cations are in the range of micro- to milliseconds, much longer than the pico- to nanosecond luminescence lifetimes that are typical for fluorescent organic molecules and proteins. For bioanalytical and imagery applications, the long luminescence lifetimes allow simple and accurate discrimination of the lanthanide complex signal from autofluorescence through time-resolved measurements (see Figure 1-10). This provides enhanced signal-to-noise ratio and significantly improved detection sensitivity.

Due to these unique properties luminescent lanthanide complexes have been used in fluoroimmunoassays, replacing radioimmunoassays.[1] For such applications luminescent

lanthanide complexes have been attached to antibodies which bind specific antigens and therefore certain cells (e.g. cancer cells).
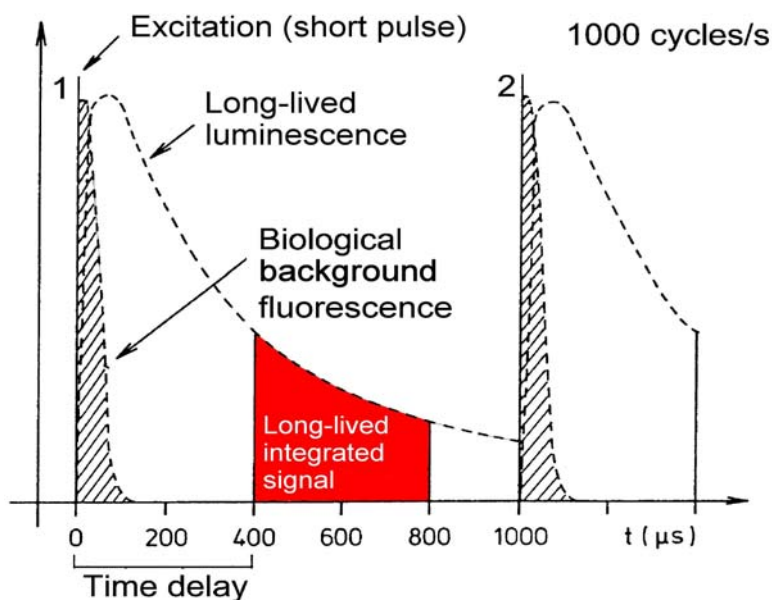
Figure 1-10: Principle of time-resolved measurement in biological applications.[7]

The metal based luminescence intensity may vary as a function of pH, pO_2 or concentration of certain bioactive cations. This means that luminescent lanthanide complexes can also be used for quantitative measurements as biosensors.[12]

In order to use luminescent lanthanide complexes in biological applications they need to have certain properties. In most of the cases the complexes can not be toxic, need to be sufficiently water-soluble, should be luminescent, thermodynamically stable and/or kinetically inert to avoid loss of luminescence signal due to the decomposition of the complex.

In order to maximize the luminescence intensity the lanthanide complexes should have high quantum yields and high extinction coefficients. The complex coordination number should be

sufficient to saturate the binding sites of the lanthanide ion (between 8 and 12 for complexes in solution), providing protection from water molecules or other quenchers.[6]

1.3 DENDRIMERS AS LIGANDS FOR LANTHANIDES

In this project we propose to evaluate a family of dendrimers as ligands for the formation of luminescent polymetallic complexes. The proposed dendrimers are several generations of PAMAM (polyamidoamine) dendrimer. The use of dendrimers provides an efficient and versatile way to increase the luminescence of the compound by incorporating larger numbers of chromophoric groups and several lanthanide cations into one discrete molecule.

Dendrimers are well defined, highly branched nanoscale molecules consisting of three different regions: *core*, radially branched layers termed *generations* and the *surface*. Dendrimers are polymers possessing three-dimensional architectures and high degree of order. The higher the dendrimer generation is, the greater the number of repeating units. There is a limit; however, as the number of units increases exponentially as a function of generation, the space available for the branches increases only as a cube of generation[13]. The dendrimers adopt globular conformations as a result of steric hindrance of the branches at the surface of the molecule. Another important characteristic of the dendrimers is the fact that they form internal cavities or channels, which enable them to encapsulate ions or small molecules. The characteristics of the dendrimer structures are depicted in Figure 1-11.

13
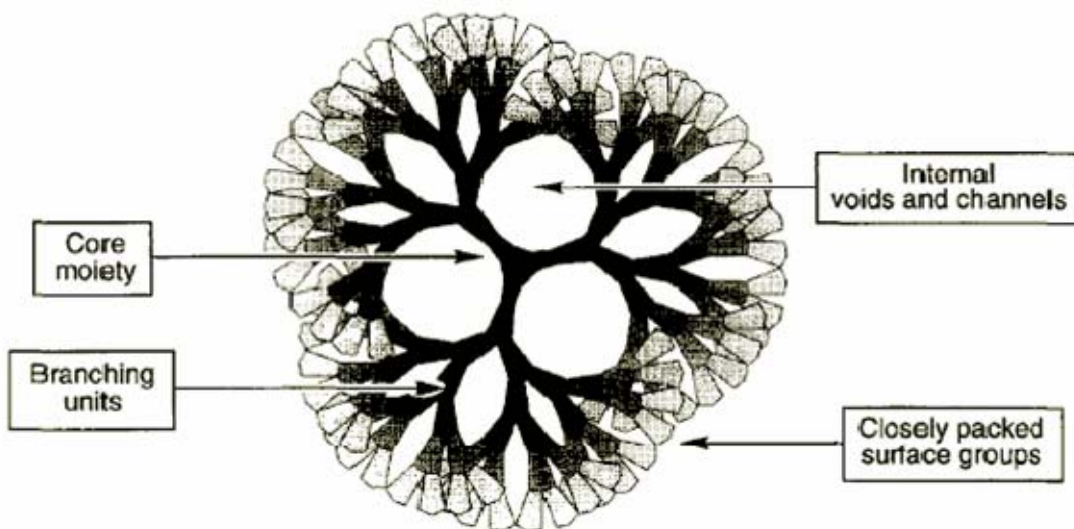
Figure 1-11: Dendritic structure demonstrating structural characteristics of this kind of molecules.[13]

The first attempt of dendrimer synthesis was done by Vögtle and co-workers at the end of the 1970s.[13] One type of dendrimers - polyamidoamine (PAMAM) - called "*starburst dendrimers*" was developed by Tomalia and his group. They are highly branched polymers with extremely low polydispersity. The name "starburst dendrimers" was introduced, after star-branched polymers and the Greek word "*dendra*" for a tree. The term "*dendrimer*" is now used almost universally to describe highly branched, monodisperse macromolecular compounds.[13]

There are two different approaches to synthesize the dendrimer molecules: *divergent* dendrimer and *convergent* dendrimer growth (Figure 1-12). In the convergent growth approach the synthesis starts from the periphery of the molecule and progresses inward by gradually linking surface units with more monomers. This method was first reported by Hawker and Fréchet.[14] In the divergent growth approach the dendrimer starts to grow outwards from the core, diverging into space. This approach was used by Tomalia, Newkome and Vögtle.[13, 15]
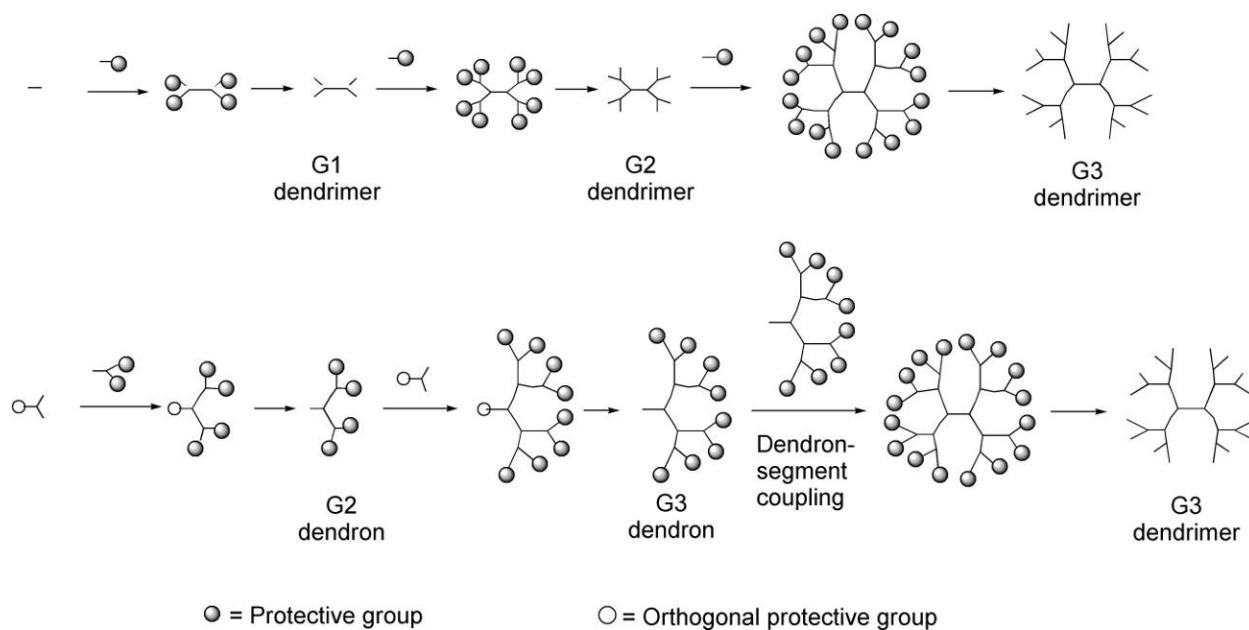
Figure 1-12: Dendrimer synthesis (schematically depicted). Top: divergent strategy. Bottom: convergent strategy.[16]

The dendrimer structure has been chosen as a basis for the formation of polymetallic lanthanide complexes. This is a simple strategy to maximize the luminescence of lanthanide complexes by coordinating a large number of lanthanide cations in the dendritic core (polymetallic) and by maximizing the extinction coefficient of the complexes due to the large number of lanthanide sensitizers bound to the end of the dendrimer branches (see Chapter 1.4). Lanthanide ions can be incorporated in each region of a dendritic structure. In our project they will be incorporated into the branches (Chapter 3). In addition, the globular structure of the dendrimer is expected to shield the lanthanide cations from molecules (such as water) that can deactivate the excited states of the lanthanide cations through non-radiative pathways. Another advantage of this strategy is that sensitizers do not need to be directly bound to the metal ion, allowing for a broader choice of lanthanide sensitizers. We have chosen polyamidoamine types of dendrimers (PAMAM) since they fulfill all of these requirements. This family of dendrimers possesses oxygen atoms from the
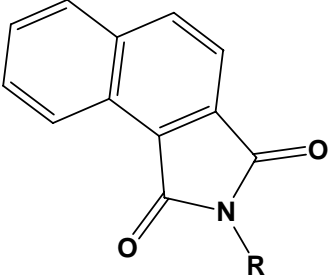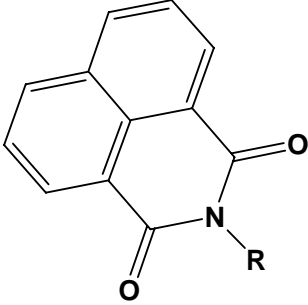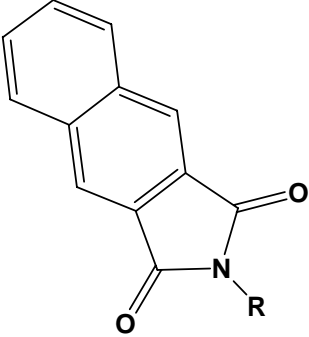
amide groups that are hard Lewis bases suitable for forming strong coordination bonds with lanthanide cations, which are hard Lewis acids. These dendrimers are commercially available in large quantities as aqueous or methanolic solutions with the branches terminated by $-NH_2$, $-OH$ or $-COOH$ groups, allowing flexibility in the addition of chromophoric groups onto these sites. In addition, these dendrimers are available in different generations from Dendritech, Michigan, (from 0 to 10 for PAMAM-NH_2 dendrimer).

1.4 NAPHTHALIMIDE SENSITIZERS

Choosing appropriate sensitizers for lanthanides that will function as antennae should be dictated by the compatibility of the donating energy level of the emitter with the accepting energy level of the lanthanide. Several naphthalimide groups, 1,2-, 2,3- and 1,8-naphthalimides (Table 1-1), have been chosen as sensitizers. The energy levels of these triplet states are compatible with the accepting energy levels of several lanthanide cations emitting in the visible and near-infrared domains, including Eu^{3+} and Nd^{3+}. These sensitizers also have highly populated triplet states[17], a favorable feature for lanthanide sensitizers since it is hypothesized that energy transfer occurs from the ligand triplet state to the accepting levels of the lanthanide cations. Therefore, high populations of the triplet state should favor efficient intramolecular ligand to lanthanide energy transfer.[1, 5, 18] Naphthalimides have an another desirable property for applications: they are sensitive to the presence of oxygen, therefore their lanthanide complexes could act as luminescent oxygen sensors.[19] A process that allows the covalent attachment of these different groups to the ends of the dendrimer branches has been described in the literature.[20]

Table 1-1   Structures and relevant properties of the three naphthalimide-type sensitizers which will be used as chromophores

N-R derivative of 1,2-naphthalimide	N-R derivative of 1,8-naphthalimide	N-R derivative Of 2,3-naphthalimide
Phosphorescence energy maximum:[a] 18 450 cm^{-1}	Phosphorescence energy maximum:[a] 18 519 cm^{-1}	Phosphorescence energy maximum:[a] 20 408 cm^{-1}

[a]The phosophorescence spectra are all structured. The maximum of the highest energy only is reported in this table. All data have been obtained from the reference[17]

2.0   EXPERIMENTAL PROTOCOL

This chapter contains instrumental descriptions and experimental procedures for all measurements performed in this project.

2.1 INSTRUMENTAL

^{1}H-NMR (300 MHz) and ^{13}C-NMR (75 MHz) spectra were recorded with a Bruker AC300 spectrometer. DMSO-D6, CD$_3$OD and CDCl$_3$ were used as solvents unless otherwise stated. δ values are quoted in ppm; coupling constants are given in Hz. Elemental analyses were performed by Atlantic Microlab, Inc. MS-ESI were measured on a Micromass Autospec and Agilent HP 1100 series LC-MSD. Thin layer chromatography was carried out on 0.25 mm GF60A silica plates. Column and Flash Chromatography were performed using silica gel (60-200 Mesh). Solvent ratios refer to volume prior to mixing. Ultrafree-15 Centrifugal Filter Units with 10,000 Dalton cut off filter were used for centrifugal separation and purification. Solvent removal and compound drying were completed using a rotary evaporator and vacuum oven (35 mmHg, 40 Celsius degree unless otherwise stated).

UV/VIS absorption spectra were recorded on a Perkin-Elmer Lambda 19 spectrophotometer coupled with personal computer using software supplied by Perkin-Elmer in 1 cm quartz cells manufactured by NSG Precision Cells, Inc. Absorbencies were converted into molar extinction

coefficients by means of equation (2-1). Results were collected as a plot of extinction coefficients versus wavelength.

$$A = \varepsilon bc \qquad (2\text{-}1)$$

Where: ε is the molar extinction coefficient, b is cell thickness and c is the molar concentration. Luminescence and phosphorescence excitation and emission spectra were collected using a Cary Eclipse coupled to a personal computer with software supplied by Varian or a modified Jobin Yvon – Spex Fluorolog-322 spectrofluorimeter equipped with cell holders for both room temperature and 77K measurements. This instrument enables measurement of radiation in both visible and NIR. Spectra were corrected for the instrumental function (excitation and emission). All measurements were taken with samples in 1 mm or 1cm quartz cells manufactured by NSG Precision Cells, Inc.

2.2 BATCH SPECTROPHOTOMETRIC TITRATION

A batch spectrophotometric titration was performed with Dend:Ln solutions in DMSO or water at 10^{-6} M, where Dend = PAMAM-1 or PAMAM-2, Ln = Eu^{3+}, Tb^{3+}, Nd^{3+}, Yb^{3+} . Solutions were prepared by diluting previously prepared stock solutions of these complexes. The following M:L ratios were used, keeping the Dend concentration constant and increasing the amount of Dend:Ln ratio 1:2, 1:4, 1:6, 1:7, 1:7.5, 1:8, 1:8.5, 1:9, 1:10, 1:12, 1:14, unless otherwise stated. The metal centered visible emission was measured using phosphorescence mode with appropriate delay time to eliminate any remaining ligand centered emission. The metal centered NIR emission was collected using a 715 nm cut off filter to block any ligand second order emission. Each spectrum was baselined, zeroed, and corrected for instrument function. The titrations were repeated over

several days to assess the formation time of the complexes. Emission intensities measured each day were compared to a control reference solution of quinine sulfate and corrected accordingly. Three batches of solution were prepared and used for measuring each Ln/PAMAM complex. The corrected emission bands were integrated using either Origin software (version 7.0) or Spex software. Plots of integrated intensity of emission versus Ln:PAMAM ratio and of integrated intensity divided by the Ln concentration versus the Ln:PAMAM ratio were drawn.

2.3 TRIPLET STATE ENERGY MEASUREMENT

2.3.1   Determination of the energy position of the ligand centered triplet state

Samples of the Gd/PAMAM and La/PAMAM complexes in anhydrous DMSO were placed in a quartz tube, which was then put into a quartz cryostat filled with liquid nitrogen. Once the sample was frozen at 77K, the cryostat sample holder was placed in the instrument, and the tube was aligned in the excitation light beam. Measurements were conducted with a Jobin-Yvon Spex Fluorolog-322 spectrofluorimeter equipped with a phosphorimeter module and Xenon flash lamp for time-resolved detection or with a Cary Eclipse. The excitation and emission spectra were collected, with increasing delay times until the phosphorescence band was the only remaining band observed on a spectrum.

2.3.2 Measurement of the triplet state luminescence lifetime

Luminescence lifetime measurements of the triplet state for complexes with PAMAM-1 were performed by excitation of solutions in quartz tube using a Nitrogen laser as a source of excitation (Oriel model 79110, wavelength 337.1 nm, pulse width at half-hight 15ns) with an external trigger allowing repetition of the laser pulse every 10-20 seconds to assure complete decay of the phosphorescence after each excitation pulse. Emission was collected at a right angle to the excitation beam, and wavelengths were selected by means of the Jobin-Yvon Spex Fluorolog-322 FL1005 double monochromator. The signal was monitored by a Hamamatsu R928 photomultiplier coupled to a 500 MHz bandpass digital oscilloscope (Tektronix TDS 620B). The signal from > 500 flashes was collected and averaged. Background signals were similarly collected and subtracted from sample signals. Luminescence lifetimes were averaged from at least three independent measurements.

2.4 LANTHANIDE LUMINESCENCE LIFETIME MEASUREMENTS

The luminescence lifetime measurements of the lanthanide emission for complexes with PAMAM-1 were performed by excitation of solutions in 1 mm quartz cells (NSG Precision Cells, Inc.) using the Nitrogen laser with internal trigger (10 Hz repetition rate). The luminescence lifetime measurements of the lanthanide emission for complexes with PAMAM-2 were performed by excitation of solutions using Neodymium YAG laser. Emission from the solution was collected at a right angle from the excitation beam by a 3" plano-convex lens. For the emission in visible range, collected emission wavelengths were selected by means of the

Jobin-Yvon Fluorolog-322 FL1005 double monochromator. The signal was monitored by a Hamamatsu R928 photomultiplier coupled to a 500 MHz bandpass digital oscilloscope (Tektronix TDS 754B). For the emission in NIR, emission wavelengths were selected means of glass filters and signal monitored by a cooled photomultiplier (Hamatsu R316) coupled to the same oscilloscope. The signal from > 500 flashes was collected and averaged. Background signals were similarly collected and subtracted from sample signals. Luminescence lifetimes were averaged from at least three independent measurements.

2.5 STEADY STATE LUMINESCENCE QUANTUM YIELD MEASUREMENTS

Metal luminescence quantum yields for visible emitting lanthanides were measured using a quinine sulfate reference (Φ = 0.546).[21] Two pairs of solutions with different absorbancies for each pair were prepared of both the unknown and the reference. Emission spectra were collected using a Jobin-Yvon Spex Fluorolog-322 Spectrofluorimeter and spectra were corrected for the instrumental function. For each sample/reference pair, the total integrated emission was measured using the same spectral parameters for each pair. The quantum yields for visible emitting lanthanides were calculated using the equation 1-1. The values of η are as follow: η = 1.333 in 0.05 M H_2SO_4, η = 1.479 in DMSO.

Metal luminescence quantum yields for NIR emitting lanthanides were measured using a neodymium (III) tropolonate reference (Φ=2.1x10^{-3}).[11] Three pairs of solutions with different absorbancies for each pair were prepared of both the unknown and the reference. For each sample/reference pair, the total integrated emission upon excitation at four different wavelengths was measured using the same spectral parameters for each pair. Plots of the total integrated

emissions (E) against absorbencies (A) yielded straight lines with slops E/A. The quantum yields (Φ_x) were calculated from the following equation 2-2:[22]

$$\Phi_x = \Phi_r \, [\text{slop}_x/\text{slop}_r] \, (\eta_x/\eta_r)^2 \qquad (2\text{-}2)$$

Where subscript *r* stands for the reference and *x* for the sample; η is the refractive index.

2.6 TIME-RESOLVED LUMINESCENCE QUANTUM YIELD MEASUREMENTS

Time-resolved luminescence quantum yields were measured using Tb(H22IAM) reference solutions in methanol, which has a known absolute quantum yield ($\Phi = 0.59$)[10] Luminescence lifetime decays and time-resolved emission spectra were collected for both the lanthanide samples and reference solutions with an excitation wavelength of 350nm. The time-resolved emission spectra were collected with a delay time of 0.1ms using the phosphorimeter module of the Jobin-Yvon Spex Fluorolog-322. The exponential decays were integrated from 0 to 25ms and from the delay time to 25ms. The 25ms value was chosen because it is a point long past any remaining luminescence for either Tb^{3+} complex. The differences in these two integrated values were used to determine the amount of luminescence intensity lost to the time-delayed measurement, using equation 2-3:

$$I_0 = [I^* \times A_0] / A^* \qquad (2\text{-}3)$$

23

where A^* is the area under the luminescence lifetime curve from the delay time to 25ms, A_0 is the area from time zero, I^* is the integrated intensity measured after the delay, and I_0 is the calculated total intensity. Once the intensities have been calculated, the quantum yield of the sample can be calculated through equation 1-1.

2.7 MEASUREMENT OF THE KINETIC OF COMPLEX FORMATION

Measurements of the kinetic of complex formation were performed using a Varian Cary Eclipse coupled to a personal computer with software supplied by Varian. The instrument was equipped with a home built thermostated cell holder and stirrer. The cuvette containing a solution of the dendrimer in anhydrous DMSO was placed in the cell holder, $Eu(NO_3)_3$ solution (in DMSO) was added and the measurement was started. Intensity of emission at the wavelength 614 nm was recorded once every hour for three weeks. Plots of emission intensity versus time were recorded.

2.8 CELL MICROINJECTION AND NEAR-INFRARED (NIR) IMAGING

This work was done in collaboration with Professors Claudette St. Croix and Simon Watkins (Center for Biological Imaging, Department of Cell Biology and Physiology, University of Pittsburgh, PA).
An IX81 Olympus microscope was used for microinjection and imaging. Detection was obtained with a cooled QIMAGING ROLERA-XR High-Performance Near-Infrared IEEE 1394 FireWire Digital CCD Camera. Both were done using a 40X oil, UplanFl, 1.3 numerical aperture

objective. Rat aortic endothelial cells (RAECs) were plated at approximately 70% confluence on single chamber Labteks (Nalge Nunce International, Naperville, IL) in phosphate free HEPES buffer maintained at 37C in an open Harvard microincubator (Harvard Apparatus, Holliston, MA). Individual RAECs were injected using an InjectMan NI2, Femtojet, and Femtotips II (all by Eppendorf North America, Westbury, NY). Injection was done using a solution of 100mg/ml Nd_8/PAMAM-2 in DMSO for 1.2 sec and an injection pressure of 180 hpa. Cells were imaged using MetaMorph 6.2 (Universal Imaging Corp, Downington, PA) using differential interference contrast (dic), and fluorescence was detected using 380 nm excitation filter and BA515IF emission filter. Cells were imaged prior to microinjection to identify any autofluorescence and then were immediately imaged after microinjection and then time-lapse imaging was obtained every 2 minutes while hypo- or hyper-oxic gas was bubbled into the media.

3.0 DENDRIMERS WITH A SINGLE TYPE OF INTERNAL COORDINATION SITE

This chapter describes the synthesis, photophysical characterizations, and biological application of selected lanthanide complexes with dendritic ligand-sensitizers based on generation 3 PAMAM Starburst dendrimers functionalized on the surface with the lanthanide sensitizer 2,3-naphthalimide to give G(3)-PAMAM-(2,3-naphthalimide)$_{32}$ abbreviated **PAMAM-1** and with 1,8-naphthalimide to give G(3)-PAMAM-(1,8-naphthalimide)$_{32}$ abbreviated **PAMAM-2**. These two compounds are examples of dendritic ligands with sensitizers on the surface of the dendrimer and coordination sites in the interior. The molecular structures are depicted in Figure 3-1 and Figure 3-2 respectively.

3.1 THEORETICAL BACKGROUND

Two different lanthanide sensitizers will be compared in their ability to perform intramolecular energy transfer and sensitization of lanthanides. This will be achieved by measuring and comparing quantum yields of the luminescence emission from PAMAM-1 and PAMAM-2 complexes with different lanthanides.

We will also evaluate the ability of these dendritic ligands to protect lanthanides from the non-radiative deactivation due to solvent molecules. This can be achieved (in addition to quantum

yield measurements) by measuring the luminescence lifetimes of the lanthanides in deuterated and non-deuterated solvents, at room and at low temperature (77K).

Another goal is the investigation of the energy conversion from the absorption of light by the ligand to the luminescence emission from lanthanide. This will allow the development of a rational approach for the application of these sensitizers as antenna.

A practical goal of this project is preparation of visible and especially NIR emitting complexes for application in biology and medicine (bioimaging, *in vivo* microscopy, in cell oxygen sensing).[16, 23] NIR photons can penetrate deep into tissues without causing damage and without significant loss of intensity owing to the low absorption of NIR photons in such media.[24]

To achieve the proposed goals, several complexes of PAMAM-1 and PAMAM-2 with lanthanides will be formed. In the second step the nature of the complexes formed in the solution will be identified. This will be done by spectrophotometric titration, which implies the monitoring of the changes of the photophysical properties of a complex with respect to varying stoichiometry. For this project the luminescence intensity arising from Ln^{3+} in complexes formed in different M:L ratio is monitored and compared. Plots of luminescence intensity at the given wavelength corresponding to lanthanide cation emission versus metal to ligand ratios will be plotted. Based on these results several complexes emitting in the visible and NIR as well as complexes formed with "silent" lanthanides (lanthanum and gadolinium) in the proper M:L ratios will be prepared and analyzed. Several absorption, excitation, and emission spectra of the free dendrimer ligands and their complexes will be recorded and analyzed. Series of quantitative measurements such as luminescence lifetimes of the ligand centered phosphorescence (luminescence lifetime of the triplet state), luminescence lifetime of the lanthanide centered luminescence as well as the quantum yields of the energy conversion will be performed and

compared. All these measurement will serve as a basis for the evaluation of the nature of the energy transfer in these complexes and the identification of the parameters which control the transfer. In the next step, the thermodynamic stability of the complexes will be evaluated in the presence of competitive ligands such as EDTA or DTPA as well as the kinetics of their formation and dissociation. These will be quantified by monitoring the lanthanide centered emission in function of time. Finally the ability of the complexes to serve as tools in biological and medical applications (cell staining, bioimaging, oxygen sensing in the cell) will be performed by *in vitro* experiments.

The europium complex of PAMAM-1 has been synthesized in our group in the form of Eu_8/PAMAM-1 and studied. Part of the preliminary results have been reported in the *Journal of the American Chemical Society* in December 2004.[25] It has been demonstrated that this dendrimer ligand is able to incorporate an average of 7.5 lanthanide cations in solution. Luminescence lifetimes of the Eu^{3+} cations recorded at room temperature (1.10 ms) and 77 K (1.16 ms) indicate that each lanthanide cation in the dendrimer is well protected from non-radiative deactivation by the dendritic structure. Despite the low efficiency of energy transfer between the chromophore and lanthanide cation (quantum yield of 0.06%), the Eu^{3+} centered emission is still visible when irradiated with a regular laboratory UV lamp ($\lambda_{ex} = 354$ nm) due to the large number of conjugated chromophoric groups (high absorbance) and luminescent cations.
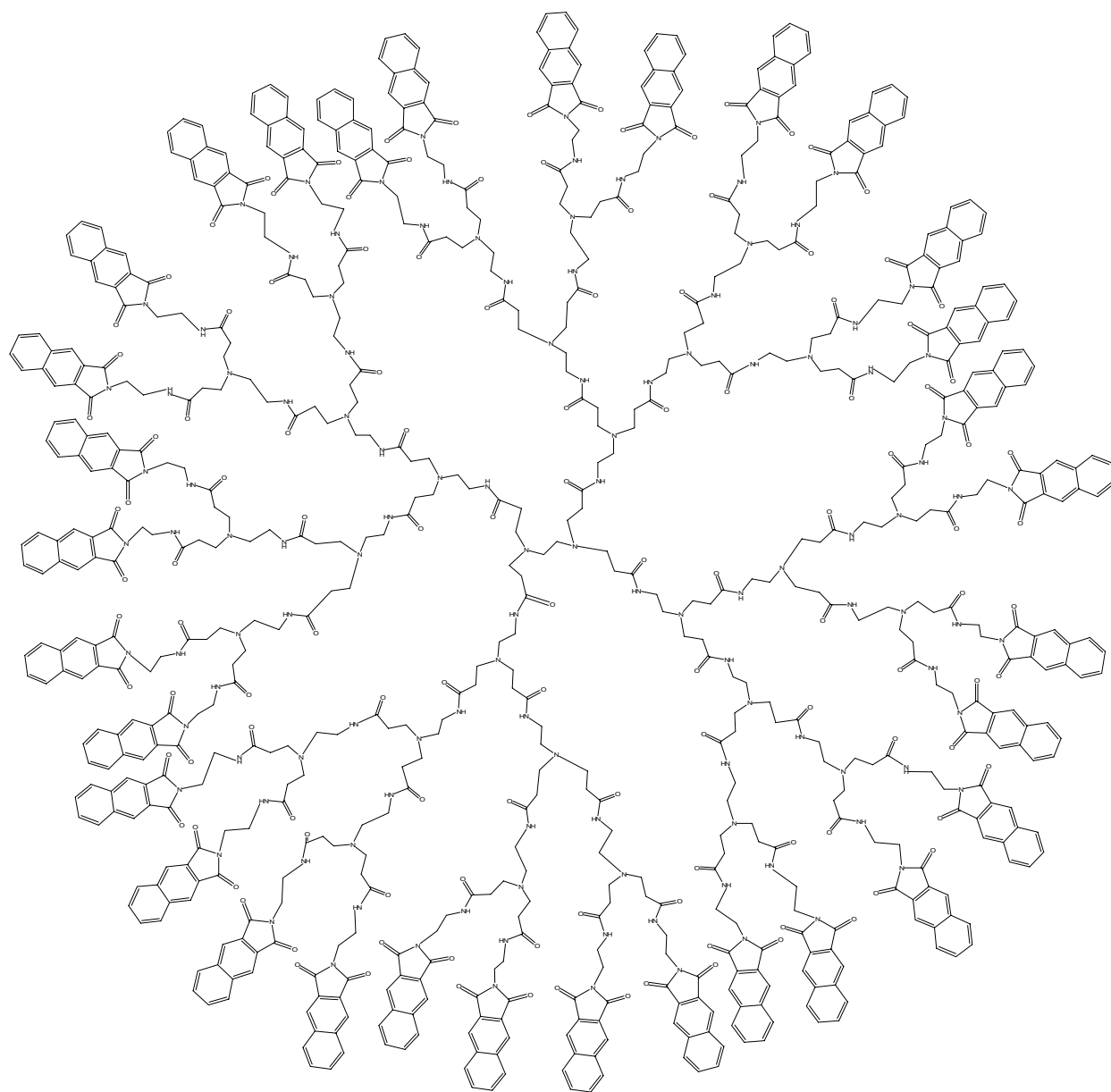
Figure 3-1 Molecular structure of G(3)-PAMAM-(2,3-naphthalimide)₃₂ abbreviated PAMAM-1
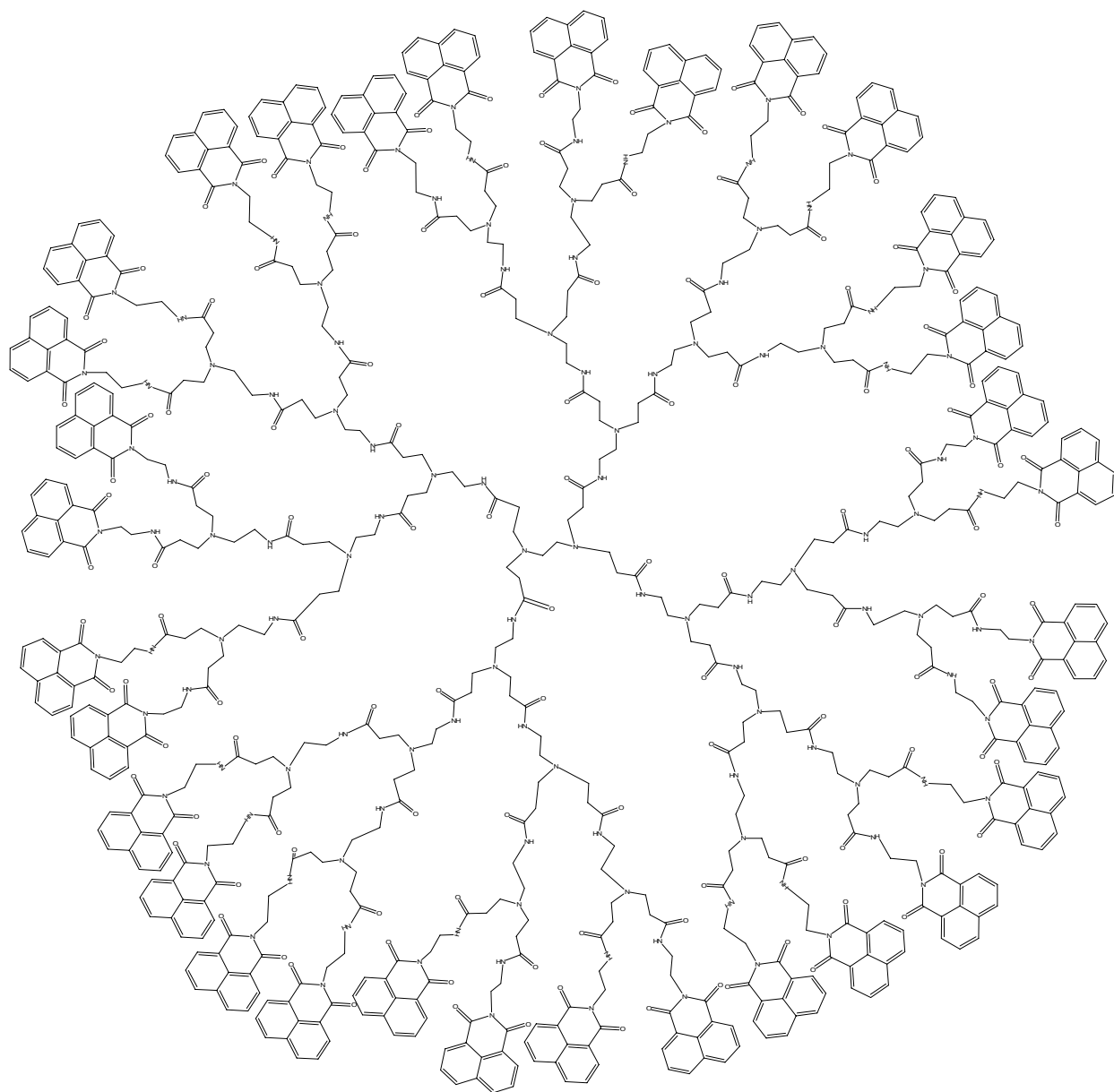
Figure 3-2 Molecular structure of G(3)-PAMAM-(1,8-naphthalimide)$_{32}$ abbreviated PAMAM-2

3.2 EXPERIMENTAL

The synthesis of the dendritic ligand-sensitizers **PAMAM-1** and **PAMAM-2** and their spectroscopic characterizations are described in this chapter.

3.2.1 Reagents

The PAMAM generation 3 dendrimer dissolved in anhydrous methanol (26.03% by weight) was purchased from Dendritech (Michigan). 2,3- naphthalic anhydride, 1,8-naphthalic anhydride and 1,2-naphthalic anhydride were purchased from TCI America (New York). Methylsulfoxide extra dry with molecular sieves and N,N-Dimethylformamide, extra dry with molecular sieves, were purchased from Acros Organics. $Ln(NO_3)_3 \cdot nH_2O$ (Ln = Tb, Er and Yb, 99.9% or 99.99%, n = 5 or 6), were purchased from Aldrich. $Ln(NO_3)_3 \cdot 6H_2O$ (Ln = Eu, Nd Gd and La, 99.9% or 99.99%) and $LnCl_3 \cdot 6H_2O$ (Ln = Pr, Sm, Dy, Ho and Tm, 99.9% or 99,99%) were bought from Strem Chemicals. Quinine sulfate (99.0%) was purchased from Fluka. All deuterated NMR solvents were purchased from Cambridge Isotope Labs and used as received.

3.2.2 Synthesis of PAMAM-1 and PAMAM-2

3.2.2.1 Synthesis of G(3)-PAMAM-(2,3-naphthalimide)$_{32}$ (PAMAM-1).

PAMAM dendrimer G(3)-NH$_2$ (0.390mg, 0.0561mmol) was treated with a 40 molar excess of 2,3-naphthalic anhydride (445mg, 2.24 mmol) while refluxing in DMF (10cm3) for 48 hours under a nitrogen atmosphere, whilst monitoring for the disappearance of the naphthalic anhydride by thin layer chromatography (silica gel). The functionalized dendrimer was obtained after removal of the solvent and trituration in toluene to yield a pale brown solid. Further purification was achieved by column chromatography (silica gel) using dichloromethane and methanol gradient (from 9:1 to 85:15) to remove any excess of 2,3-naphthalic anhydride. The title compound was isolated as a pale brown flocculent solid (689mg, 96%); Found C, 62.16; H, 6.28; N, 12.45, C$_{686}$H$_{736}$N$_{122}$O$_{124}$*32H$_2$O Requires C, 62.18; H, 6.09; N, 12.9; UV/Vis (DMSO) λ_{max} (ϵ/dm3 mol-1cm-1) 263 nm (202,040), 342 nm (55,320) and 360 nm (74,300); ν_{max} (Nujol/cm-1) 3430 (broad, N-H), 2867, 2733, 1730 (C=O), 1726 (C=O), 1622, 1583, 1370, 1251 and 1148; 1H-NMR [300MHz; (CD$_3$)$_2$SO] 2.09-2.57 (180 H, broad s, N(CH$_2$)$_3$), 3.09 (60 H, broad s, NH), 3.31 (120 H, broad s, -CH$_2$NHCO), 3.54 (120 H, broad s, NCO-CH$_2$), 3.62 (64H, broad s, N(CO)$_2$-CH$_2$) 7.67 (64H, broad s, 1-H and 4-H), 8.09 (64H, broad s, 5-H and 8-H), 8.54 (64H, broad s, 6-H and 7-H), 13C-NMR [75MHz; (CD$_3$)$_2$SO], 31.28, 32.96, 34.68, 37.64, 38.96, 64.40, 66.29, 68.18, 127.88 (ArC) , 128.96 (ArC), 130.02 (ArC), 131.12 (ArC), 134.80 (ArC), 167.40 (NHCO), 171.54 [N(CO)$_2$].

3.2.2.2 Synthesis of G(3)-PAMAM-(1,8-naphthalimide)$_{32}$ (PAMAM-2).

Synthetic procedure and quantities are the same as for PAMAM-1. Dark brown solid was obtained (539mg, 75%). This work was accomplished by Dr. Jason Cross – a former member of our research group.

3.2.3   Photophysical properties of the PAMAM-1 and PAMAM-2 dendrimers

Stock solution of 4.991×10^{-3} M PAMAM-1 was prepared by dissolving 12.65 mg in 200.0 µl of anhydrous DMSO (water content 130ppm). Stock solution of 4.785×10^{-3} M PAMAM-2 was prepared by dissolving 12.13 mg in 200.0 µl of anhydrous DMSO (130ppm of water).

3.2.3.1 UV/VIS absorption spectra, Molar Absorption Coefficients

Stock solution of 4.991×10^{-3} M PAMAM-1 and stock solution of 4.785×10^{-3} M PAMAM-2 were diluted 1000 times with anhydrous DMSO (130ppm of water) to the concentration 10^{-6} and used to collect UV/Vis absorption spectra.

3.2.4 Preparation of Nd^{3+}/PAMAM-1 complexes in different ratios and batch Spectrophotometric Titration

Ln^{3+}/PAMAM-1 complexes were prepared in different ratios to investigate which is the most luminescent species by batch spectrophotometric titration. The titration was performed and fluorescence emission spectra were collected as described in experimental part (Chapter 2.2).

Stock solutions of 1.11×10^{-5} M PAMAM-1 (5ml) and 1.82×10^{-4} Nd(NO$_3$)$_3$*6H$_2$O (5ml) in anhydrous DMSO (130ppm H$_2$O) were prepared and used to obtain batch 1 of Nd^{3+}/PAMAM-1 complexes in several ratios. All complexes were diluted with anhydrous DMSO to the final concentration 1.11×10^{-6} M and volume 5ml.

Table 3-1: Preparation of Nd^{3+} /PAMAM-1 complexes for spectrophotometric titration - batch 1.

Batch 1 Complex #	Dendrimer stock sol. (c= 1.11E-5 mol/l) Volume in [μl]	Nd^{3+} to dendrimer Ratio	Nd(NO$_3$)$_3$ stock sol. (c= 1.82E-4 mol/l) Volume in [μl]	Solvent (DMSO) Volume in [ml]
1	500	0	0	4.500
2	500	4	155	4.345
3	500	6	232	4.268
4	500	7	270	4.230
5	500	8	309	4.191
6	500	9	347	4.153
7	500	10	386	4.114
8	500	12	464	4.036

Stock solutions of 1.58×10^{-5} M PAMAM-1 (5ml) and 6.71×10^{-4} Nd(NO$_3$)$_3$*6H$_2$O (5ml) in anhydrous DMSO (130ppm H$_2$O) were prepared and used to obtain batch 2 of Nd^{3+}/PAMAM-1 complexes in several ratios. All complexes were diluted with anhydrous DMSO to the final concentration 1.58×10^{-6} M and volume 5ml.

Table 3-2: Preparation of Nd^{3+}/PAMAM-1 complexes for spectrophotometric titration - batch 2

Batch 2 Complex #	Dendrimer stock sol (c= 1.58 E-5 mol/l) Volume in [μl]	Nd^{3+} to dendrimer Ratio	Nd(NO$_3$)$_3$ stock sol. (c= 6.71 E-4 mol/l) Volume in [μl]
1	500	0	0
2	500	6	70.6
3	500	7	82.4
4	500	8	94.1
5	500	9	105.9
6	500	10	117.7

Stock solutions of 1.67×10^{-5} M PAMAM-1 dendrimer (5ml) and 6.77×10^{-4} Nd(NO$_3$)$_3$*6H$_2$O (5ml) in anhydrous DMSO (130ppm H$_2$O) were prepared and used to obtain batch 3 of Nd^{3+}/PAMAM-1 complexes in several ratios. All complexes were diluted with anhydrous DMSO to the final concentration 1.67×10^{-6} M and volume 5ml.

Table 3-3: Preparation of Nd^{3+}/PAMAM-1 complexes for spectrophotometric titration - batch 3.

Batch 3 Complex #	Dendrimer stock sol (c= 1.67E-5 mol/l) Volume in [μl]	Nd^{3+} to dendrimer Ratio	Nd(NO$_3$)$_3$ stock sol. (c= 6.77E-4 mol/l) Volume in [μl]
1	500	0	0.0
2	500	6	74.0
3	500	7	86.3
4	500	7.5	92.5
5	500	8	98.7
6	500	8.5	104.8
7	500	9	111.0
8	500	10	123.3

3.2.5   Measurement of the kinetic of complex formation

A Stock solution of 1.669×10^{-5} M PAMAM-1 in anhydrous DMSO (43ppm H_2O) was prepared by dissolving 2.116 mg in 10 ml. Similarly a stock solution of 5.847×10^{-4} M Eu^{3+} was prepared by dissolving 2.608 mg of $Eu(NO_3)_3*6H_2O$ in 10 ml anhydrous DMSO. 2 ml of PAMAM-1 stock solution was placed in a cell. 456.8 µl of Eu^{3+} stock solution was added to obtain the 1.669×10^{-6} M Eu_8/PAMAM-1 complex. Luminescence intensity was recorded every hour for 3 weeks in time-resolved mode. Experimental set-up: λ_{ex} 332 nm, λ_{em} 614 nm, excitation slit 10, emission slit 10, averaging time 0.005 s, total decay time 0.02 s, number of flashes 1, delay time 0.2 ms, gate time 5 ms.

3.2.6   Preparation of the Gd₈/PAMAM-1 and La₈/PAMAM-1 complexes and investigation of the singlet and triplet energy state

Gd_8/PAMAM-1 and La_8/PAMAM-1 complexes were prepared for investigation of the singlet and triplet energy state levels in the PAMAM-1 complexes with non-luminescent lanthanides ions (Gd^{3+} and La^{3+}). All measurements were performed as described in the experimental protocol (Chapter 2).

3.2.6.1   Incubation of PAMAM-1 with Gd³⁺ and Ln³⁺ ions in the ratio 1:8

A Stock solution of 2.160×10^{-4} M PAMAM-1 in anhydrous DMSO (198ppm H_2O) was prepared by dissolving 27.38 mg in 10.00 ml. Stock solutions of 5.13×10^{-3} M Gd^{3+} and 5.21×10^{-3} M La^{3+} were prepared from nitrate salts and used to obtain Gd/PAMAM-1 and La/PAMAM-1 complexes in the ratio 8:1. Both complexes were diluted with anhydrous DMSO to the final concentration 2.16×10^{-5} M and volume 5.00 ml.

Table 3-4: Preparation of the Gd$_8$/PAMAM-1 and La$_8$/PAMAM-1 complexes

Sample #	Dendrimer stock sol 2.160E-04 Volume in [ml]	Ln^{3+} to dendrimer Ratio	Gd(NO$_3$)$_3$ stock sol. 5.13E-03 Volume in [μl]	Final Concentration mol/l
1	0.500	8	168.32	2.16E-05
	Dendrimer stock sol 2.160E-04		La(NO$_3$)$_3$ stock sol. 5.21E-03	
2	0.500	8	165.90	2.16E-05

3.2.6.2   UV/VIS absorption spectra, Molar Extinction Coefficients

Complexes prepared as described above were diluted 10 times to the concentration 2.16x10^{-6} M (5.00 ml) and used to collect UV-Vis absorption spectra at 25°C in the range of 260 nm – 700 nm. Anhydrous DMSO was used as spectral reference.

3.2.6.3   Excitation and emission spectra at 295K and 77K – measurement of the position of the S$_1$ and T$_1$ energy state

Excitation and emission spectra were collected on the complexes prepared as described above (3.2.6.1). The positions of the ligand singlet state energy level (steady-state) and triplet state energy level (time-resolved mode) were investigated. The following instrumental set-up was used for the measurements: scan start 340 nm, scan end 800 nm (1 nm increment), λ_{ex} 330 nm, excitation slits 10, emission slits 8, sample window (SW): 5.0 ms, time per flash (TPF): 5000 ms, number of flashes (NF): 20, and delay after flash (DAF): 0.01-1.0 ms.

3.2.6.4   Measurement of the luminescence lifetime of T$_1$ at 77K

The luminescence lifetime of the triplet state luminescence was measured as described in Chapter 2. The following instrumental parameters were used: λ_{ex} 337.1 nm (Nitrogen laser), λ_{em} 484 nm (for Gd$_8$/PAMAM-1) and λ_{em} 520 nm (for La$_8$/PAMAM-1), emission slit 10.

3.2.7 Preparation of Ln$_8$/PAMAM-1 complexes (where Ln = Eu^{3+}, Sm^{3+}, Tb^{3+}, Dy^{3+}, Nd^{3+}, Yb^{3+}, Pr^{3+}, Er^{3+}, Ho^{3+}, Tm^{3+}) and photophysical characterization.

Complexes of PAMAM-1 with several different lanthanide ions were prepared for an investigation of their photophysical properties. All measurements were performed as described in the experimental protocol (Chapter 2).

3.2.7.1 Incubation of PAMAM-1 with Ln^{3+} ions in the ratio 1:8

A Stock solution of 2.160×10^{-4} M PAMAM-1 in anhydrous DMSO (198ppm H$_2$O) was prepared by dissolving 27.38 mg in 10.00 ml. Stock solutions of Ln^{3+} (10^{-3} M) were prepared from nitrate or chloride salts and used to obtain series of Ln/PAMAM-1 complexes in the ratio 8:1 (M:L). All complexes were diluted with anhydrous DMSO to the final concentration of 2.16×10^{-5} M and total volume of 5.00 ml. The total concentration of Ln^{3+} ions in each complex solution was 1.73×10^{-4} M. A set of lanthanide solutions in DMSO were prepared without dendrimers so that the lanthanide concentrations were identical (1.73×10^{-4} M) to those of the Ln/PAMAM-1 solutions. This set of solutions serves as control set for comparison with batch 1 of complexes (blank solution).

Table 3-5: Preparation of the Ln$_8$/PAMAM-1 complexes - batch 1

Batch 1 Complex #	Dendrimer stock sol 2.160E-04 M Volume in [ml]:	Ln^{3+} to dendrimer Ratio	Eu(NO$_3$)$_3$ stock sol. 5.562E-03 M Volume in [µl]:	Final Concentr. mol/l
1	0.500	8	155.3	2.16E-05
	Dendrimer stock sol 2.160E-04		Tb(NO$_3$)$_3$ stock sol. 6.320E-03	
2	0.500	8	136.7	2.16E-05
	Dendrimer stock sol 2.160E-04		SmCl$_3$ stock sol. 5.606E-03	
3	0.500	8	154.1	2.16E-05
	Dendrimer stock sol 2.160E-04		DyCl$_3$ stock sol. 4.996E-03	
4	0.500	8	172.9	2.16E-05
	Dendrimer stock sol 2.160E-04		Nd(NO$_3$)$_3$ stock sol. 5.743E-03	
5	0.500	8	150.4	2.16E-05
	Dendrimer stock sol 2.160E-04		Er(NO$_3$)$_3$ stock sol. 5.107E-03	
6	0.500	8	169.2	2.16E-05
	Dendrimer stock sol 2.160E-04		HoCl$_3$ stock sol. 5.706E-03	
7	0.500	8	151.4	2.16E-05
	Dendrimer stock sol 2.160E-04		PrCl$_3$ stock sol. 5.106E-03	
8	0.500	8	169.2	2.16E-05
	Dendrimer stock sol 2.160E-04		TmCl$_3$ stock sol. 4.939E-03	
9	0.500	8	174.9	2.16E-05
	Dendrimer stock sol 2.160E-04		Yb(NO$_3$)$_3$ stock sol. 4.878E-03	
10	0.500	8	177.1	2.16E-05

A stock solution of 2.550×10^{-4} M PAMAM-1 in anhydrous DMSO (130ppm H$_2$O) and stock solutions of Ln^{3+} (10^{-3} M) prepared from nitrate salts were used to obtain Ln/PAMAM-1 complexes in the ratio 8:1. All complexes were diluted with anhydrous DMSO to the final concentration 2.55×10^{-5} M and volume 5.00 ml.

Table 3-6: Preparation of the Ln₈/PAMAM-1 complexes - batch 2.

Batch 2 Complex #	Dendrimer stock sol 2.550E-04 Volume in [ml]	Ln^{3+} to dendrimer Ratio	Eu(NO$_3$)$_3$ stock sol. 5.562E-03 Volume in [ml]	Molar Concentr. mol/l
1	0.500	8	0.18339	2.55E-05
	Dendrimer stock sol 2.550E-04		Nd(NO$_3$)$_3$ stock sol. 5.743E-03	
2	0.500	8	0.17761	2.55E-05

3.2.7.2 UV/VIS absorption spectra, Molar Extinction Coefficients

Solutions of 2.550x10^{-5} M Eu₈/PAMAM-1 and Nd₈/PAMAM-1 complexes prepared as described above (batch 2) were diluted to the final concentration of 2.550x10^{-6} M with anhydrous DMSO (130ppm H$_2$O) and used to collect UV/Vis absorption spectra.

3.2.7.3 Excitation and emission spectra

Solutions of 2.16x10^{-5} M Ln₈/PAMAM-1 complexes prepared as described above (batch 1) were used without further dilution to collect excitation and emission spectra. Similarly solutions of lanthanide salts prepared as described above were used without further dilution to collect excitation and emission spectra. The following instrumental parameters were used for the measurements: λ_{ex} 330 nm, λ_{em} 615 nm, excitation and emission slits: 2, 2 (for Eu₈/PAMAM-1 and Eu(NO$_3$)$_3$), λ_{ex} 330 nm, λ_{em} 543 nm, excitation and emission slits: 5, 5 (for Tb₈/PAMAM-1 and Tb(NO$_3$)$_3$), λ_{ex} 330 nm, λ_{em} 600 nm, excitation and emission slits: 14, 14, SW: 5, DAF: 0.03, TPF: 50, NF: 20 (for Sm₈/PAMAM-1 and SmCl$_3$), λ_{ex} 330 nm, λ_{em} 1523 nm, excitation and emission slits: 14, 40 (for Er₈/PAMAM-1 and Er(NO$_3$)$_3$), λ_{ex} 330 nm, λ_{em} 980 nm, excitation and emission slits: 14, 40 (for Ho₈/PAMAM-1 and HoCl$_3$), λ_{ex} 330 nm, λ_{em} 800 nm, excitation and emission slits: 14, 40 for (for Tm₈/PAMAM-1 and TmCl$_3$), λ_{ex} 330 nm, λ_{em} 980 nm, excitation

and emission slits: 10, 10 (for Yb_8/PAMAM-1 and $Yb(NO_3)_3$), λ_{ex} 330 nm, λ_{em} 1024 nm, excitation and emission slits: 14, 40 for (for Pr_8/PAMAM-1 and $PrCl_3$), λ_{ex} 330 nm, λ_{em} 1065 nm, excitation and emission slits: 10, 40 (for Nd_8/PAMAM-1 and $Nd(NO_3)_3$). A 715 nm cut off filter was used for all NIR emitting complexes.

Similarly solutions of 2.550×10^{-5} M Eu_8/PAMAM-1 and Nd_8/PAMAM-1 complexes prepared as described above (batch 2) were used without further dilution to collect excitation and emission spectra in the visible part of the spectrum for comparison. The following instrumental set-up was used for the measurements: λ_{ex} 360 nm, λ_{em} 390 nm, excitation and emission slits: 1.5, 1.5.

3.2.7.4   Lifetime of the Ln^{3+} luminescence in the complexes

Solutions of 2.16×10^{-5} M Nd_8/PAMAM-1 and Sm_8/PAMAM-1 complexes prepared as described above (batch 1) were used without further dilution to measure the luminescence lifetime of the lanthanide luminescence as described in Chapter 2. The following instrumental set-up was used for the measurements: λ_{ex} 337 nm (Nitrogen laser), λ_{em} 1060 nm (for Nd_8/PAMAM-1) and λ_{em} 595 nm (for Sm_8/PAMAM-1).

3.2.8   Preparation of Ln^{3+}/PAMAM-2 complexes in different ratios and batch spectrophotometric titration

Formation of the most luminescent species was monitored through a batch spectrophotometric titration of Ln^{3+}/PAMAM-2 complexes in different ratios. The titration was performed and fluorescence emission spectra were collected as described in experimental part (Chapter 2).

3.2.8.1 Batch Spectrophotometric Titration of Eu^{3+}/PAMAM-2

Stock solutions of 5.60×10^{-5} M PAMAM-2 (15ml) and 5.50×10^{-4} M $Eu(NO_3)_3 \cdot 6H_2O$ (15ml) in anhydrous DMSO (130ppm H_2O) were prepared and used to obtain batch 1 of Eu^{3+}/PAMAM-2 complexes in several ratios. All complexes were diluted with anhydrous DMSO to the final concentration 5.60×10^{-6} M and 10ml volume.

Table 3-7: Preparation of Eu^{3+}/PAMAM-2 complexes for spectrophotometric titration - batch 1.

Batch 1 Sample #	Dendrimer stock sol 5.60E-05 Volume in [µl]	Eu^{3+} to dendrimer Ratio	$Eu(NO_3)_3$ stock sol. 5.50E-04 Volume in [µl]
1	1000	2	203.6
2	1000	4	407.3
3	1000	6	610.9
4	1000	6.5	661.8
5	1000	7	712.7
6	1000	7.5	763.6
7	1000	8	814.5
8	1000	8.5	865.5
9	1000	9	916.4
10	1000	9.5	967.3
11	1000	10	1018.2
12	1000	11	1120.0
13	1000	12	1221.8

Stock solutions of 5.50×10^{-4} M PAMAM-2 (1ml) and 5.56×10^{-3} $Eu(NO_3)_3 \cdot 6H_2O$ (1ml) in anhydrous DMSO (130ppm H_2O) were prepared and used to obtain batch 2 of Eu^{3+}/PAMAM-2 complexes in several ratios. All complexes were diluted with anhydrous DMSO to the final concentration 5.50×10^{-5} M and 10ml volume.

Table 3-8: Preparation of Eu³⁺ /PAMAM-2 complexes for spectrophotometric titration - batch 2.

Batch 2 Sample #	Dendrimer stock sol 5.50E-04 Volume in [μl]	Eu³⁺ to dendrimer Ratio	Eu(NO₃)₃ stock sol. 5.56E-03 Volume in [μl]
1	100	2	19.78
2	100	4	39.55
3	100	6	59.33
4	100	6.5	64.28
5	100	7	69.22
6	100	7.5	74.16
7	100	8	79.11
8	100	8.5	84.05
9	100	9	89.00

Stock solutions of 5.68×10^{-5} M PAMAM-2 (15ml) and 5.04×10^{-4} Eu(NO₃)₃*6H₂O (15ml) in anhydrous DMSO (130ppm H₂O) were prepared and used to obtain batch 3 of Eu³⁺/PAMAM-2 complexes in several ratios. All complexes were diluted with anhydrous DMSO to the final concentration 5.68×10^{-6} M and 10ml total volume.

Table 3-9: Preparation of Eu³⁺ /PAMAM-2 complexes for spectrophotometric titration - batch 3.

Batch 3 Sample #	Dendrimer stock sol 5.68E-05 Volume in [μl]	Eu³⁺ to dendrimer Ratio	Eu(NO₃)₃ stock sol. 5.04E-04 Volume in [μl]
1	1000	2	225.41
2	1000	4	450.81
3	1000	6	676.22
4	1000	6.5	732.57
5	1000	7	788.92
6	1000	7.5	845.28
7	1000	8	901.63
8	1000	8.5	957.98
9	1000	9	1014.33
10	1000	9.5	1070.68
11	1000	10	1127.03
12	1000	11	1239.74

3.2.8.2 Batch spectrophotometric titration of Tb^{3+}/PAMAM-2

Stock solutions of 5.70×10^{-5} M PAMAM-2 (15 ml) and 5.78×10^{-4} $Tb(NO_3)_3 \cdot 6H_2O$ (15 ml) in anhydrous DMSO (130ppm H_2O) were prepared and used to obtain batch 1 of Tb^{3+}/PAMAM-2 complexes in several ratios. All complexes were diluted with anhydrous DMSO to the final concentration 5.70×10^{-6} M and 10 ml volume.

Table 3-10: Preparation of Tb^{3+}/PAMAM-2 complexes for spectrophotometric titration - batch 1.

Batch 1 Sample #	Dendrimer stock sol 5.70E-05 Volume in [μl]	Tb^{3+} to dendrimer Ratio	$Tb(NO_3)_3$ stock sol. 5.78E-04 Volume in [μl]
1	1000	2	197.1
2	1000	4	394.2
3	1000	6	591.3
4	1000	6.5	640.6
5	1000	7	689.8
6	1000	7.5	739.1
7	1000	8	788.4
8	1000	8.5	837.6
9	1000	9	886.9
10	1000	9.5	936.2
11	1000	10	985.5
12	1000	11	1084.0
13	1000	12	1182.6

Stock solutions of 5.57×10^{-5} M PAMAM-2 (15ml) and 6.32×10^{-3} $Tb(NO_3)_3 \cdot 6H_2O$ (15ml) in anhydrous DMSO (130ppm H_2O) were prepared and used to obtain batch 2 of Tb^{3+}/PAMAM-2 complexes in several ratios. All complexes were diluted with anhydrous DMSO to the final concentration 5.57×10^{-6} M and 10ml volume.

Table 3-11: Preparation of Tb³⁺ /PAMAM-2 complexes for spectrophotometric titration - batch 2.

Batch 2 Sample #	Dendrimer stock sol 5.57E-05 Volume in [μl]	Tb³⁺ to dendrimer Ratio	Tb(NO₃)₃ stock sol. 6.32E-04 Volume in [μl]
1	1000	2	176.16
2	1000	4	352.31
3	1000	6	528.47
4	1000	6.5	572.50
5	1000	7	616.54
6	1000	7.5	660.58
7	1000	8	704.62
8	1000	8.5	748.66
9	1000	9	792.70
10	1000	9.5	836.74
11	1000	10	880.78
12	1000	11	968.85
13	1000	12	1056.93
14	1000	13	1145.01
15	1000	14	1233.09
16	1000	15	1321.16

Stock solutions of 5.79×10^{-5} M PAMAM-2 (15ml) and 6.22×10^{-3} Tb(NO₃)₃*6H₂O (15ml) in anhydrous DMSO (130ppm H₂O) were prepared and used to obtain batch 3 of Tb³⁺/PAMAM-2 complexes in several ratios. All complexes were diluted with anhydrous DMSO to the final concentration 5.79×10^{-6} M and 10ml volume.

Table 3-12: Preparation of Tb³⁺ /PAMAM-2 complexes for spectrophotometric titration - batch 3.

Batch 3 Sample #	Dendrimer stock sol 5.79E-05 Volume in [μl]	Tb³⁺ to dendrimer Ratio	Tb(NO₃)₃ stock sol. 6.22E-04 Volume in [μl]
1	1000	2	186.24
2	1000	4	372.48
3	1000	6	558.71
4	1000	6.5	605.27
5	1000	7	651.83
6	1000	7.5	698.39
7	1000	8	744.95
8	1000	8.5	791.51
9	1000	9	838.07
10	1000	9.5	884.63
11	1000	10	1024.31
12	1000	11	1117.43

3.2.8.3   Batch Spectrophotometric Titration of Nd³⁺ /PAMAM-2

Stock solutions of 5.106×10^{-5} M PAMAM-2 (10ml) and 9.580×10^{-4} Nd(NO₃)₃*6H₂O (5ml) in anhydrous DMSO (130ppm H₂O) were prepared and used to obtain batch 1 of Nd³⁺/PAMAM-2 complexes in several ratios. All complexes were diluted with anhydrous DMSO to the final concentration 5.106×10^{-6} M and 5 ml volume.

Table 3-13: Preparation of Nd^{3+} /PAMAM-2 complexes for spectrophotometric titration - batch 2.

Batch 1 Sample #	Dendrimer stock sol. 5.106E-05 M Volume in [μl]	Nd^{3+} to dendrimer Ratio	Nd(NO$_3$)$_3$ stock sol. 9.580E-04 M Volume in [μl]
1	500	2	53.3
2	500	4	106.6
3	500	6	159.9
4	500	6.5	173.2
5	500	7	186.5
6	500	7.5	199.9
7	500	8	213.2
8	500	8.5	226.5
9	500	9	239.8
10	500	9.5	253.2
11	500	10	266.5
12	500	11	293.1
13	500	12	319.8

Stock solutions of 4.785x10^{-5} M PAMAM-2 (5 ml) and 1.1910x10^{-3} Nd(NO$_3$)$_3$*6H$_2$O (5 ml) in anhydrous DMSO (50ppm H$_2$O) were prepared and used to obtain batch 2 of Nd^{3+}/PAMAM-2 complexes in several ratios. All complexes were diluted with anhydrous DMSO to the final concentration 4.785x10^{-6} M and 5 ml volume.

Table 3-14: Preparation of Nd^{3+} /PAMAM-2 complexes for spectrophotometric titration - batch 3.

Batch 2 Sample #	Dendrimer stock sol 4.785E-05 M Volume in [μl]	Nd^{3+} to dendrimer Ratio	Nd(NO$_3$)$_3$ stock sol. 1.191E-03 M Volume in [μl]
1	500	6	120.5
2	500	7	140.6
3	500	7.5	150.7
4	500	8	160.7
5	500	8.5	170.7
6	500	9	180.8
7	500	10	200.9

Stock solutions of 4.785x10^{-5} M PAMAM-2 (5 ml) and 1.1910x10^{-3} Nd(NO$_3$)$_3$*6H$_2$O (5 ml) in anhydrous DMSO (50ppm H$_2$O) were prepared and used to obtain batch 3 of Nd^{3+}/PAMAM-2

complexes in several ratios. All complexes were diluted with anhydrous DMSO to the final concentration 4.785×10^{-6} M and 5 ml volume.

3.2.9 Preparation of the Gd$_8$/PAMAM-2 complex and investigation of the location of the singlet and triplet energy state

A Gd$_8$/PAMAM-2 complex was prepared for the investigation of the position of the singlet and triplet energy state of the PAMAM-2 in complex with the non-luminescent lanthanide ion, gadolinium. All measurements were performed as described in the experimental protocol (Chapter 2).

3.2.9.1 Incubation of PAMAM-2 with Gd^{3+} ions in the ratio 1:8.

A Stock solution of 2.160×10^{-4} M PAMAM-2 in anhydrous DMSO (130ppm H$_2$O) was prepared by dissolving 27.35 mg in 10.00 ml. Stock solutions of 5.13×10^{-3} M Ln^{3+} were prepared from nitrate salts and used to obtain complex of Gd/PAMAM-2 in the ratio 8:1. The complex was diluted with anhydrous DMSO to the final concentration 2.16×10^{-5} M and volume 5.00 ml.

Table 3-15: Preparation of the Gd$_8$/PAMAM-2 complex

Sample	Dendrimer stock sol 2.160E-04 Volume in [ml]	Ln^{3+} to dendrimer Ratio	Gd(NO$_3$)$_3$ stock sol. 5.13E-03 Volume in [μl]	Final Concentration mol/l
1	0.500	8	168.32	2.16E-05

3.2.9.2   UV/VIS absorption spectra, Molar Extinction Coefficients

Complexes prepared as described above were diluted 10 times to the concentration 2.16×10^{-6} M (5.00 ml) and used to collect UV-Vis absorption spectra. UV-Vis absorption spectra were collected at 25^{0}C in the range of 260 nm – 700 nm for each of these solutions using anhydrous DMSO as blank and reference.

3.2.9.3   Excitation and emission spectra at 295K and 77K – measurement of the position of the S_1 and T_1 energy states

The complex prepared as described above (3.2.9.1) was used without further dilution to collect excitation and emission spectra to investigate the energetic position of the ligand singlet state energy level (fluorescence mode, 295K) and triplet state energy level (time-resolved mode, 77K). The following instrumental parameters were used for the measurements: λ_{ex} 300 nm, scan start 310 nm, scan end 600 nm (1 nm increment), excitation slits: 10, emission slits: 10, SW: 2.0 ms, TPF: 500 ms, NF: 20, and DAF: 0.01, 0.05, 0.1, 0.2, 0.5, and 1.0 ms (for the higher energy triplet state) and λ_{ex} 408 nm, scan start 420 nm, scan end 800 nm (2 nm increment), excitation slits: 10, emission slits: 8, SW: 2.0 ms, TPF: 500 ms, NF: 20, and DAF: 0.01, 0.05, 0.1, 0.2, 0.5, and 1.0 ms (for the lower energy triplet state).

3.2.10 Preparation of Ln_8/PAMAM-2 complexes (where $Ln = Eu^{3+}, Sm^{3+}, Tb^{3+}, Nd^{3+}, Yb^{3+}$) and photophysical characterization.

Complexes of PAMAM-2 with several lanthanide ions were prepared for the investigation and comparison of their photophysical properties. All measurements were performed as described in the experimental protocol (Chapter 2).

3.2.10.1 Incubation of PAMAM-2 with Ln^{3+} ions in the ratio 1:8

A Stock solution of 2.160×10^{-4} M PAMAM-2 in anhydrous DMSO (130ppm H_2O) was prepared by dissolving 27.35 mg in 10.00 ml. Stock solutions of Ln^{3+} (10^{-3} M) were prepared from nitrate or chloride salts and used to obtain series of Ln/PAMAM-1 complexes in the ratio 8:1. All complexes were diluted with anhydrous DMSO to the final concentration 2.16×10^{-5} M and volume 5.00 ml.

Table 3-16: Preparation of the Ln_8/PAMAM-2 complexes - batch 1.

Batch 1 Complex #	Dendrimer stock sol 2.160E-04 M Volume in [ml]:	Ln^{3+} to dendrimer Ratio	Eu(NO₃)₃ stock sol. 5.562E-03 M Volume in [µl]:	Final Concentr. mol/l
1	0.500	8	155.3	2.16E-05
	Dendrimer stock sol 2.160E-04		Tb(NO₃)₃ stock sol. 6.320E-03	
2	0.500	8	136.7	2.16E-05
	Dendrimer stock sol 2.160E-04		SmCl₃ stock sol. 5.606E-03	
3	0.500	8	154.1	2.16E-05
	Dendrimer stock sol 2.160E-04		DyCl₃ stock sol. 4.996E-03	
4	0.500	8	172.9	2.16E-05
	Dendrimer stock sol 2.160E-04		Er(NO₃)₃ stock sol. 5.107E-03	
5	0.500	8	169.2	2.16E-05
	Dendrimer stock sol 2.160E-04		HoCl₃ stock sol. 5.706E-03	
6	0.500	8	151.4	2.16E-05
	Dendrimer stock sol 2.160E-04		PrCl₃ stock sol. 5.106E-03	
7	0.500	8	169.2	2.16E-05
	Dendrimer stock sol 2.160E-04		TmCl₃ stock sol. 4.939E-03	
8	0.500	8	174.9	2.16E-05
	Dendrimer stock sol 2.160E-04		Yb(NO₃)₃ stock sol. 4.878E-03	
9	0.500	8	177.1	2.16E-05

A Stock solution of 4.785×10^{-3} M PAMAM-2 in anhydrous DMSO (130ppm H_2O) was prepared by dissolving 12.13 mg in 200.0 µl. Stock solutions of Nd^{3+} (8.240×10^{-2} M) were prepared from nitrate salts and used to obtain 3.27×10^{-3} M Nd_8/PAMAM-2 complexes in the ratio 8:1. All complexes were diluted with anhydrous DMSO to the final concentration 3.27×10^{-5} M and volume 5.00 ml.

Table 3-17: Preparation of the Ln_8/PAMAM-2 complexes - batch 2.

Batch 2	Dendrimer stock sol 4.785E-03 Volume in [ml]	Ln^{3+} to dendrimer Ratio	$Nd(NO_3)_3$ stock sol. 8.240E-02 Volume in [ml]	Molar Concentr. mol/l
1	0.150	8	0.06968	3.27E-03

3.2.10.2   UV/VIS absorption spectra, Molar Extinction Coefficients

Solutions of 2.160×10^{-5} M Eu_8/PAMAM-2 and 3.27×10^{-5} M Nd_8/PAMAM-2 complexes prepared as described above (batch 1 and 2) were diluted to the final concentration 2.160×10^{-6} M and 3.27×10^{-6} M respectively with anhydrous DMSO (130ppm H_2O) and their UV/Vis absorption spectra were collected.

3.2.10.3   Excitation and emission spectra

Solutions of 2.16×10^{-5} M Eu_8/PAMAM-1 and Tb_8/PAMAM-2 complexes prepared as described above (batch 1) were used after dilution to 2.16×10^{-6} M to collect excitation and emission spectra. Similarly, solution of 3.27×10^{-5} M Nd_8/PAMAM-2 complex prepared as described above (batch 2) was used after dilution to 3.27×10^{-6} M to collect excitation and emission spectra. The following instrumental set-up was used for the measurements: λ_{ex} 300 nm, λ_{em} 615 nm, excitation and emission slits: 1.5, 1.5 (for Eu_8/PAMAM-2), λ_{ex} 296 nm, λ_{em} 543 nm, excitation

and emission slits: 2, 2 (for Tb$_8$/PAMAM-2) and λ_{ex} 412 nm, λ_{em} 1060 nm, excitation and emission slits: 10, 40 (for Nd$_8$/PAMAM-2).

3.2.10.4   Lifetime of the Ln^{3+} luminescence in the complexes

Solutions of 2.16x10^{-5} M Eu$_8$/PAMAM-2 and Tb$_8$/PAMAM-2 complexes prepared as described above (Batch 1) and solution of 3.27x10^{-5} M Nd$_8$/PAMAM-2 complex (batch 2) were used without further dilution to measure the luminescence lifetime of the lanthanide luminescence as described in Chapter 2. The following instrumental parameters were used for the measurements: λ_{ex} 337.1 nm (Nitrogen laser), λ_{em} 615 nm (for Eu$_8$/PAMAM-2), λ_{em} 543 nm (for Tb$_8$/PAMAM-2) and λ_{em} 1060 nm (for Nd$_8$/PAMAM-2).

3.2.10.5   Quantum yields measurements

The quantum yield for Tb$_8$/PAMAM-2 was measured in the time-resolved mode using Tb(H22IAM) as a reference (see Chapter 2.6). The following experimental parameters were used: slits 14,14, NF 3, SW 10 ms, DAF 0.1 ms, TPF 50 ms, reference sample A, B: $\lambda_{abs.}$ 350, 353, 355nm, terbium complex sample A, B: $\lambda_{abs.}$ 360, 363, 365 nm (for Tb$_8$/PAMAM-2).

The quantum yield for Eu$_8$/PAMAM-2 was measured in the steady state mode using quinine sulfate as a reference (see Chapter 2.5). The following experimental set-up was used: reference sample A,B: $\lambda_{abs.}$ 345, 350, 353, 355 nm, europium complex sample A, B: $\lambda_{abs.}$ 290, 295, 298, 305 nm.

The quantum yield for Nd$_8$/PAMAM-2 was measured in steady state mode using neodymium tropolonate complex as a reference (see Chapter 2.5). The following experimental parameters

were used for reference samples A,B,C and neodymium tropolonate samples A, B,C: $\lambda_{abs.}$ 328.36

nm, 347.10 nm, 358.88 nm, 445.55 nm.

3.2.11 Application of selected complexes in biological systems - Cell microinjection and imaging in the NIR

Stock solutions of $1.05.x10^{-3}$ M PAMAM-2 and $8.240x10^{-2}$ M $Nd(NO_3)_3$ were prepared in anhydrous DMSO (130ppm H2O) and used to prepare $9.54x10^{-4}$ M Nd_8/PAMAM-2 complex (~0.5 ml).

Table 3-18: Preparation of the Nd_8/PAMAM-2 complexes for cell microinjection and NIR imaging.

Complex #	Dendrimer stock sol 1.050E-03 Volume in [ml]	Nd^{3+} to dendrimer Ratio	$Nd(NO_3)_3$ stock sol. 8.240E-02 Volume in [ml]	Molar Concentr. mol/l
1	0.500	8	0.0510	9.54E-4

The complex was incubated for one week and micro-injected as a concentrated solution into a living rat lung endothelial cell. Oxygen sensitivity of the complex in the cell was monitored by measuring the changes in luminescence emission intensity in NIR. Oxygen concentration was varied during the experiment from 1.5% to 60%. General experimental conditions are provided in the experimental protocol (Chapter 2).

3.3 RESULTS AND DISCUSSIONS

3.3.1   UV/VIS absorption spectra of the PAMAM-1 and PAMAM-2 dendrimers

Absorption of two different naphthalimide groups attached to the PAMAM dendrimer (2,3-naphthalimides attached to PAMAM-1 and 1,8-naphthalimides to PAMAM-2) induce distinctive spectroscopic properties dependent from the position of the dicarboximide group on the naphthalene ring.[17] Because these dendrimers have low solubility in water all solutions in this project were prepared in anhydrous DMSO. PAMAM-1 solution in anhydrous DMSO gives three absorption bands, one very intense: λ_{max} (DMSO)/nm ($\varepsilon/dm^3 mol^{-1}\ cm^{-1}$) 269 (472,300) with a shoulder on the lower energy side of the band 295 (163,500) and two less absorbing: 342 (59,100) and 360 (79,100). PAMAM-2 in DMSO solution show one intense band λ_{max} (DMSO)/nm ($\varepsilon/dm^3 mol^{-1}\ cm^{-1}$): 335 (288,500) with shoulders on both higher and lower energy sides of the band and one very weak at around 400 nm. Stronger absorption at low energy for PAMAM-2 is an advantageous situation for bioanalytical application. The spectra of both PAMAM-1 and PAMAM-2 are depicted in Figure 3-3:
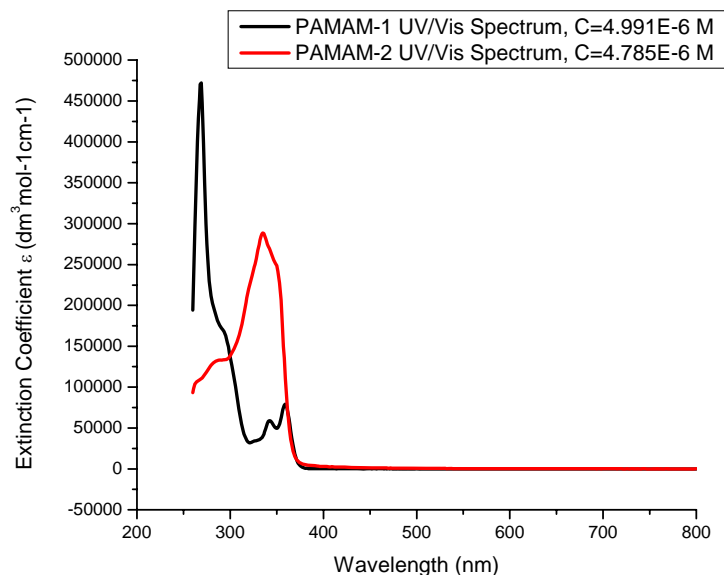
Figure 3-3: UV/Vis absorption spectra of PAMAM-1 and PAMAM-2 solutions in anhydrous DMSO at 295 K

3.3.2 Characterization of the species formed in solution and spectroscopic properties of the Ln/PAMAM-1 complexes

3.3.2.1 Batch spectrophotometric titration

Preliminary experiments have shown that PAMAM-1 forms complexes with Eu^{3+} ions in the average ratio of 7.5 (M:L).[25] This suggests that the dendritic ligand PAMAM-1 will form complexes with other lanthanides at the same ratio. Nevertheless there is a difference in size of the Ln^{3+} ions. To verify this hypothesis we have chosen Nd^{3+} ions. Europium (III) and Neodymium (III) with CN=8 differ in ionic radii (Ln^{3+}: 1.109 Å and Eu^{3+}: 1.004 Å).[26] Several batches of neodymium complexes with PAMAM-1 in different ratios were prepared to perform batch spectroscopic titration as described in the experimental section (Chapter 2.2).The results

confirmed that PAMAM-1 forms complexes with neodymium nitrate with the most luminescent species at the average ratio of 7.5 (M:L). Graphs illustrating these results are depicted in Figure 3-4 and Figure 3-5.
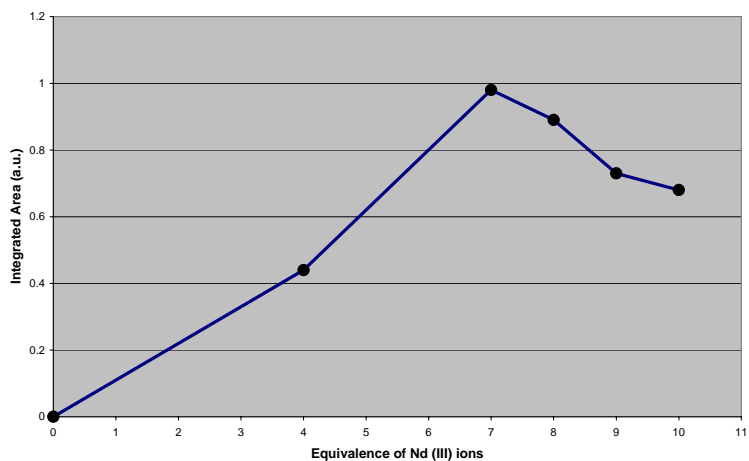
Figure 3-4: Plot of integrated intensity of Nd^{3+} emission versus the metal to ligand ratio (batch 1).
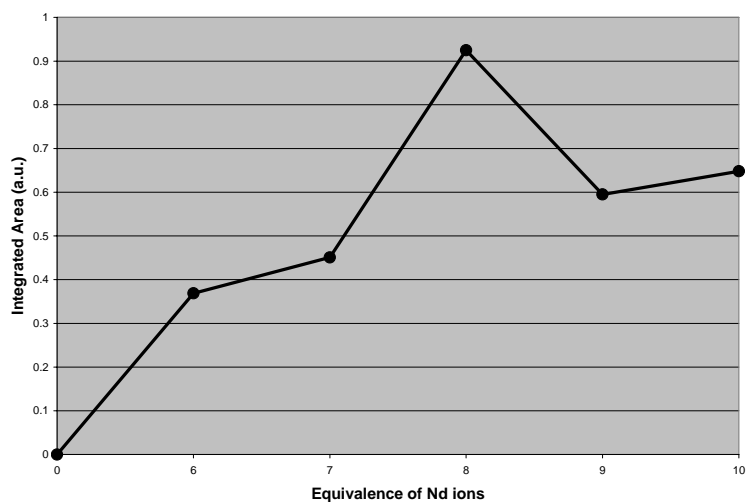
Figure 3-5: Plot of integrated intensity of Nd^{3+} emission versus the metal to ligand ratio (batch 2).

As it was mentioned in the Chapter 1, Ln^{3+} ions can accept coordination numbers between 8 and 12. Since the molecule of PAMAM-1 dendrimer possesses 60 oxygen atoms, one molecule could bind 7 ions with coordination number 8, which would use 56 and leave 4 oxygen atoms not coordinated (or 8 ions with coordination number 7). Another possible arrangement would be 8 bonded ions, where 4 of them would have coordination number 7 and the other 4 would have coordination number 8, utilizing a total of 60 oxygen sites. At this stage it was not possible to clearly identify whether there is one species or mixture of two species in the solution. It has been assumed that PAMAM-1 coordinates 8 Ln^{3+} ions in the solution and all further experiments and measurements were performed using M:L ratio 8. The following general formula for the lanthanide complexes with PAMAM-1 was proposed: Ln_8/PAMAM-1.

Batch spectroscopic titration repeated for the same set of complexes over several days revealed changes of the emission intensity with time. This observation indicates that the complex is formed slowly. The most luminescent species is not formed instantaneously after mixing the dendrimer solution with a lanthanide salt, but forms within some period of time.

3.3.2.2 Measurement of the complex formation kinetics

To assess the time necessary for the full formation of the most luminescent complex, one complex in the M:L ratio 1:8 was chosen to monitor the emission intensity of Eu(III) during three weeks from the moment of mixing as described in Chapter 2.7. This experiment revealed that 7 days are needed for full formation of this complex (Figure 3-6). Small decrease of emission intensity was observed after this time (~5% within 2 weeks).
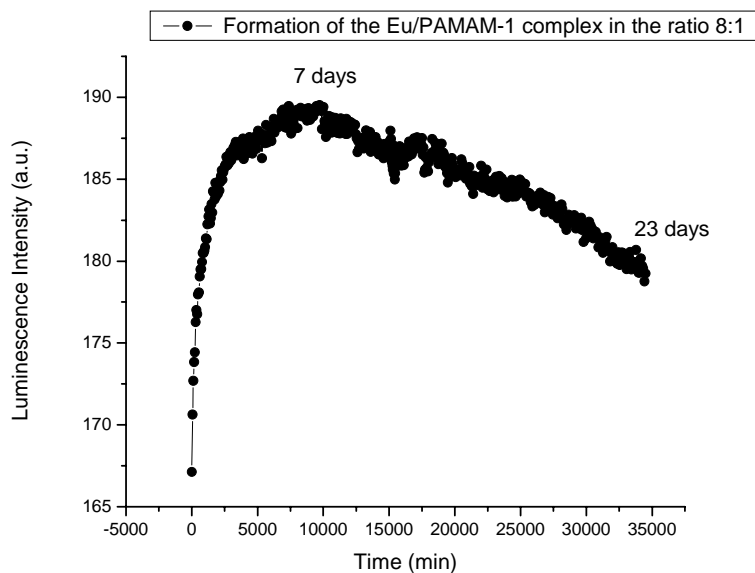
Figure 3-6: Measurement of the time required for the formation of the most luminescent Ln/PAMAM-1 complex (Eu$_8$/PAMAM-1), C=1.669x10^{-6} M, λ_{ex} 332 nm, λ_{em} 614 nm, 298 ^{0}C.

3.3.2.3 Excitation and Emission spectra

PAMAM-1 can sensitize a large number of lanthanide cations emitting in visible and NIR. Series of Ln$_8$/PAMAM-1 complex solutions in anhydrous DMSO together with a series of lanthanide (III) salts (see Ch. 3.2.7.) were prepared to investigate if PAMAM-1 form luminescent complexes with other ions than Eu^{3+}or Nd^{3+}. The concentration of Ln^{3+} ions was identical in all solutions. The results depicted in Figure 3-7 through Figure 3-15 show that in addition to Eu^{3+}, PAMAM-1 is able to sensitize Pr^{3+}, Nd^{3+}, Sm^{3+}, Tb^{3+}, Ho^{3+}, Er^{3+}, Tm^{3+} and Yb^{3+}. This is surprising since all the lanthanide ions have different accepting energy levels.

Emission Spectra: Nd(NO$_3$)$_3$ vs. Nd$_8$/PAMAM-1
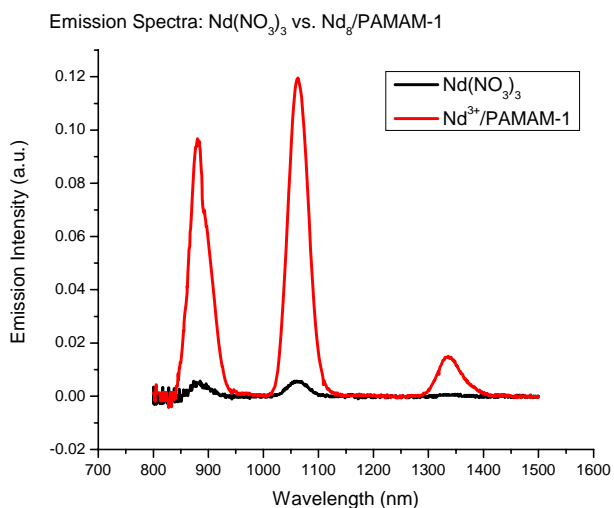
Figure 3-7: Comparison of the emission intensity of Nd$_8$/PAMAM-1 solution in anhydrous DMSO with the emission intensity of Nd(NO$_3$)$_3$ solution in anhydrous DMSO. Measurements were performed at the same experimental conditions. Concentration of the Nd^{3+} ions (1.73x10-4 M) was identical in both solutions. λ$_{ex}$: 330 nm

Emission Spectra: Yb(NO$_3$)$_3$ vs. Yb$_8$/PAMAM-1
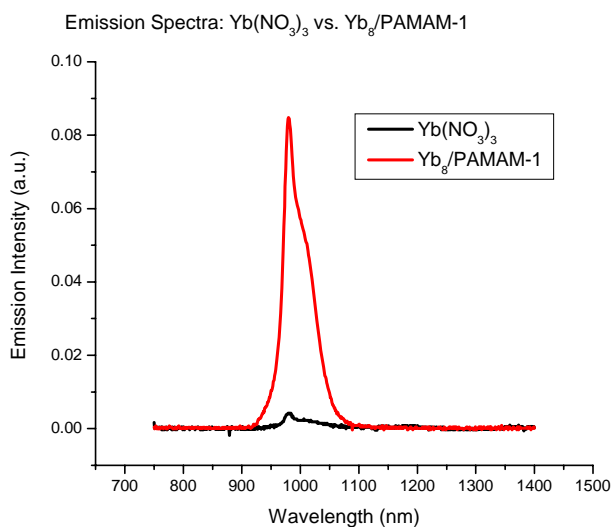
Figure 3-8: Comparison of the emission intensity of Yb$_8$/PAMAM-1 solution in anhydrous DMSO with the emission intensity of Yb(NO$_3$)$_3$ solution in anhydrous DMSO. Measurements were performed at the same experimental conditions. Concentration of the Yb^{3+} ions (1.73x10-4 M) was identical in both solutions. λ$_{ex}$: 330 nm

Emission Spectra: Er(NO$_3$)$_3$ vs. Er$_8$/PAMAM-1
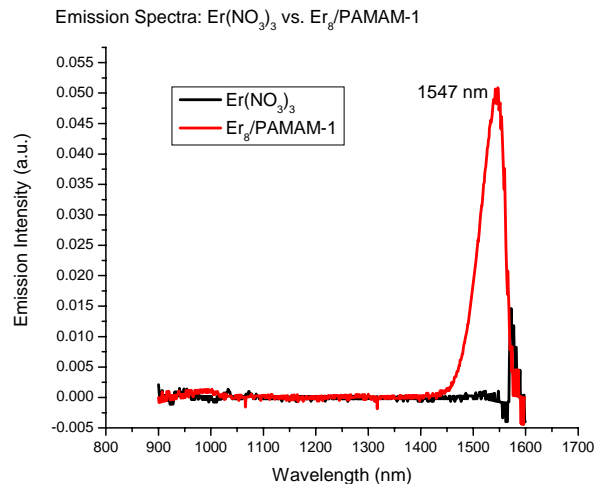
Figure 3-9: Comparison of the emission intensity of Er$_8$/PAMAM-1 solution in anhydrous DMSO with the emission intensity of Er(NO$_3$)$_3$ solution in anhydrous DMSO. Measurements were performed at the same experimental conditions. Concentration of the Er^{3+} ions (1.73x10-4 M) was identical in both solutions. λ_{ex}: 330 nm

Emission Spectra: TmCl$_3$ vs. Tm$_8$/PAMAM-1

Figure 3-10: Comparison of the emission intensity of Tm$_8$/PAMAM-1 solution in anhydrous DMSO with the emission intensity of TmCl$_3$ solution in anhydrous DMSO. Measurements were performed at the same experimental conditions. Concentration of the Tm^{3+} ions (1.73x10-4 M) was identical in both solutions. λ_{ex}: 330 nm
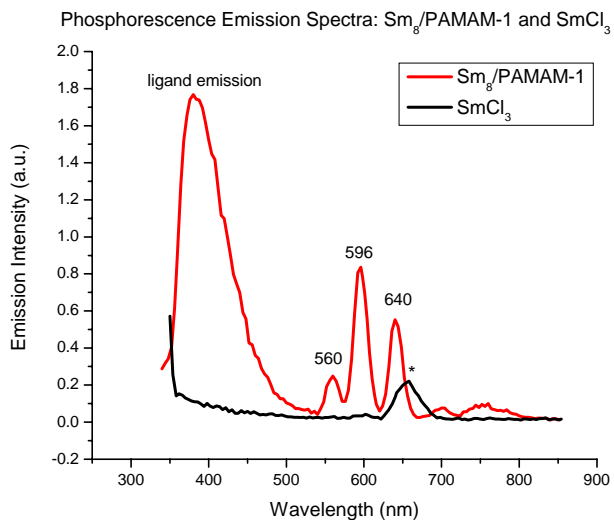
Figure 3-11: Comparison of the emission intensity of Sm$_8$/PAMAM-1 solution in anhydrous DMSO with the emission intensity of SmCl$_3$ solution in anhydrous DMSO. Measurements were performed at the same experimental conditions. Concentration of the Sm^{3+} ions (1.73x10-4 M) was identical in both solutions. λ_{ex}: 330 nm
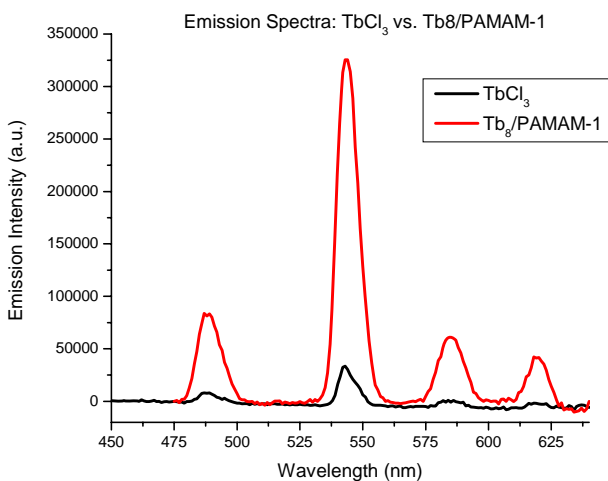
Figure 3-12: Comparison of the emission intensity of Tb$_8$/PAMAM-1 solution in anhydrous DMSO with the emission intensity of TbCl$_3$ solution in anhydrous DMSO. Measurements were performed at the same experimental conditions. Concentration of the Tb^{3+} ions (1.73x10-4 M) was identical in both solutions. λ_{ex}: 330 nm

Emission Spectra: PrCl₃ vs. Nd₈/PAMAM-1
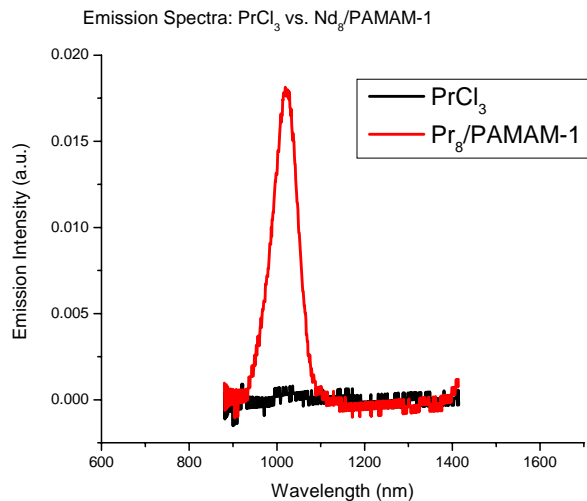
Figure 3-13: Comparison of the emission intensity of Pr₈/PAMAM-1 solution in anhydrous DMSO with the emission intensity of PrCl₃ solution in anhydrous DMSO. Measurements were performed at the same experimental conditions. Concentration of the Pr³⁺ ions (1.73x10-4 M) was identical in both solutions. λₑₓ: 330 nm
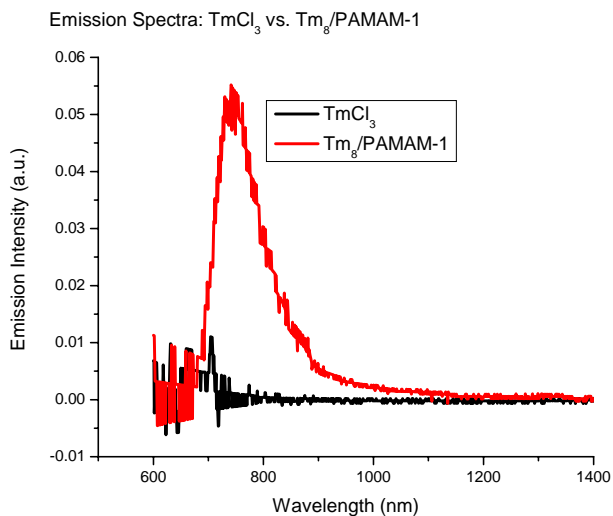

Emission Spectra: HoCl₃ vs. Ho₈/PAMAM-1
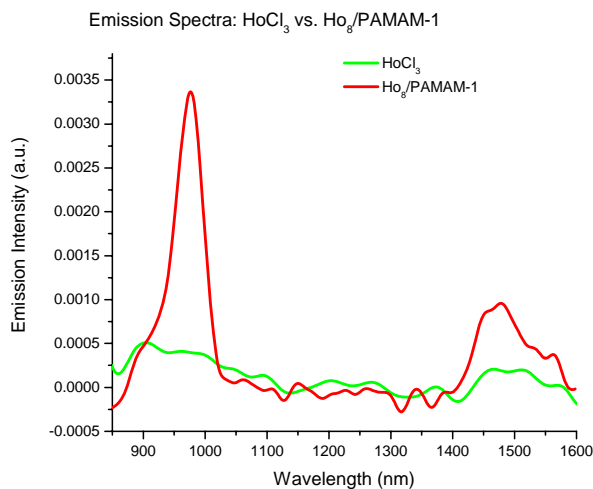
Figure 3-14: Comparison of the emission intensity of Ho₈/PAMAM-1 solution in anhydrous DMSO with the emission intensity of HoCl₃ solution in anhydrous DMSO. Measurements were performed at the same experimental conditions. Concentration of the Ho³⁺ ions (1.73x10-4 M) was identical in both solutions. λₑₓ: 330 nm
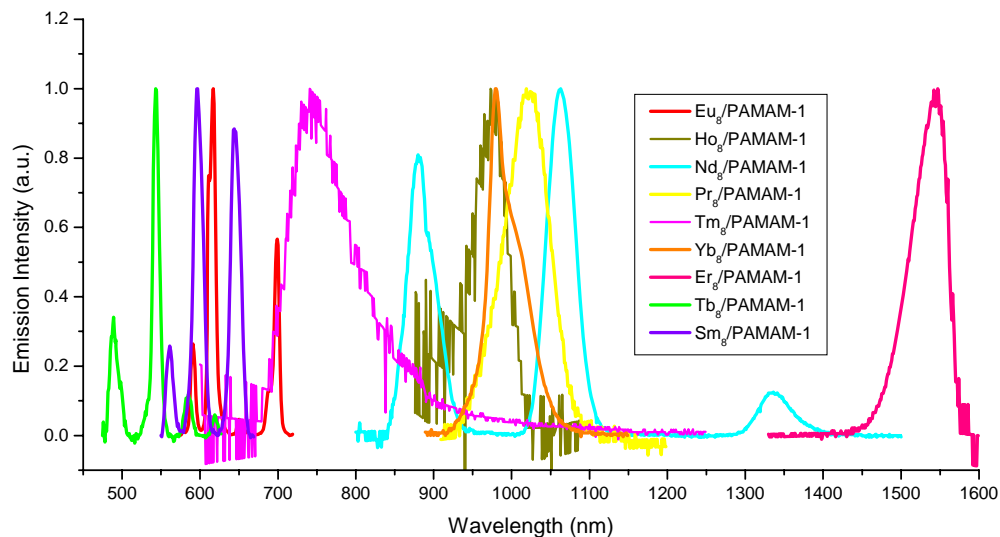
Figure 3-15: Normalized emission spectra of all prepared Ln$_8$/PAMAM-1 complexes in anhydrous DMSO (C=2.16E-5 M). λ_{ex}: 330 nm.

Direct comparison of the excitation spectra of the Ln$_8$/PAMAM-1 complexes (Figure 3-16 and Figure 3-17) revealed that they all have a common excitation band with a maximum centered at 330 nm. This is an additional confirmation that all the lanthanides are excited from the same electronic transition centered on the naphthalimide sensitizer. Direct excitation of the lanthanides would result in different excitation spectra reflecting the specific energy levels for each lanthanide.

Some of the lanthanide complexes have additional excitation maxima, indicating that sensitization of the lanthanides may occur through more than one pathway. Further investigation will be necessary to elucidate the pathways of the energy conversion in these complexes.
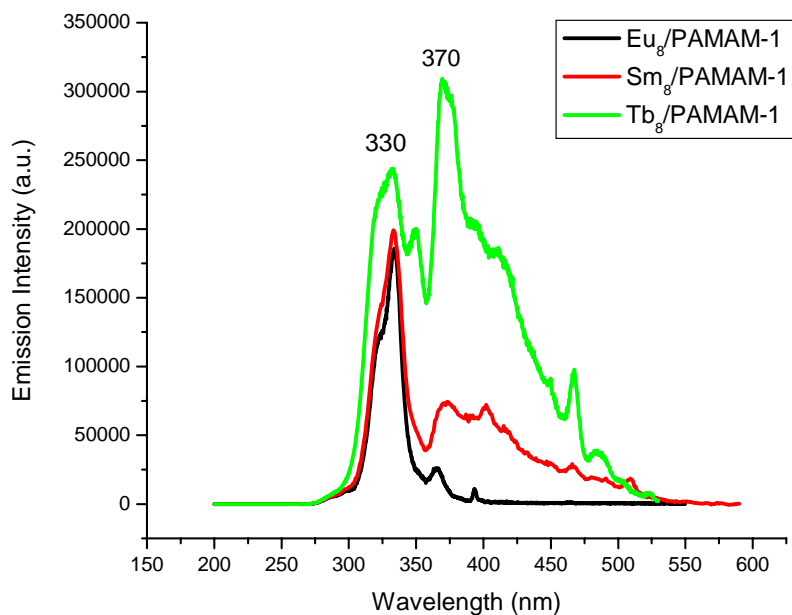
Figure 3-16: Excitation spectra of Ln$_8$/PAMAM-1 complexes emitting in visible. C=2.16E-5 M.
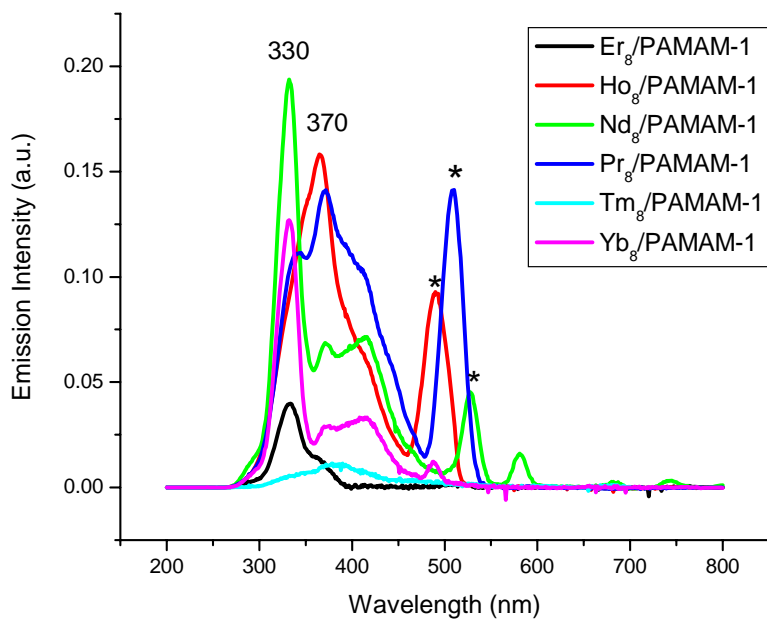
Figure 3-17: Excitation spectra of Ln$_8$/PAMAM-1 complexes emitting in NIR. C=2.16E-5 M. "*" indicate 2nd order signal generated by the grating.

3.3.2.4 UV/VIS absorption spectroscopy of the complexes

The UV/Vis absorption spectra of several complexes Ln_8/PAMAM-1 show no significant differences in the maxima positions of the absorption bands compared to uncoordinated PAMAM-1. The Ln_8/PAMAM-1 have the most intense absorption band centered at 266 nm with shoulder at lower energy (295 nm) and two bands of low intensity at 342 nm and 360 nm. The extinction coefficients differ between the free dendrimer and its complexes with lanthanides. The difference is especially pronounced for the absorption band located at the highest energy (Figure 3-18). The extinction coefficients are collected in the Table 3-19.

Table 3-19: Extinction coefficients (ε) for Ln_8/PAMAM-1 complexes

	Extinction coefficients ε/dm^{3}mol^{-1} cm^{-1}		
	at 266 nm	at 342 nm	at 360 nm
PAMAM-1	472,300	59,100	79,100
Nd$_8$/PAMAM-1	709,900	63,510	81,110
Gd$_8$/PAMAM-1	801,400	62,630	79,400
La$_8$/PAMAM-1	773,700	66,440	83,430

These extinction coefficient (ε) values are relatively large in comparison to small organic chromophores[27] due to the presence of 32 chromophoric groups attached to one molecule. This fact can be used to increase luminescent emission intensity of the lanthanides, which is proportional not only to the quantum yield of the energy conversion but also to the value of ε (see Chapter 3.5) and the number of Ln cations. The similarity between the absorption spectra can be explained by the absence of direct interaction of lanthanide ions with the 2,3-

naphthalimide moiety. If the lanthanide ions bound directly to the sensitizer moiety, changes in the absorption spectrum would probably be observed.

PAMAM-1 Set UV/Vis Specta

Legend:
- PAMAM-1, C=4.991E-6 M
- La$_8$/PAMAM-1, C=2.16E-6 M
- Nd$_8$/PAMAM-1, C=2.16E-6 M
- Gd$_8$/PAMAM-1, C=2.55E-6 M

y-axis: Extinction Coefficient ε(dm^{3}mol^{-1}cm^{-1})
x-axis: Wavelength (nm)
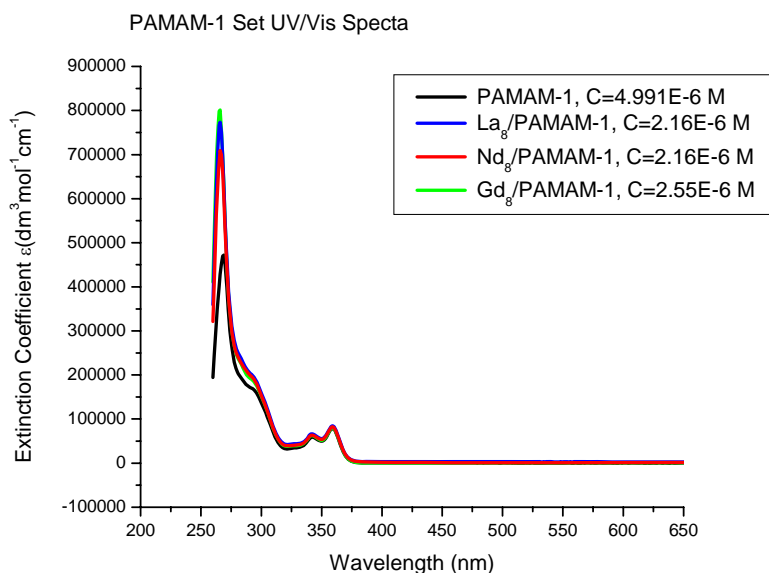
Figure 3-18: UV/Vis absorption spectra of PAMAM-1 and selected Ln$_8$/PAMAM-1 solutions in anhydrous DMSO at 295 K

3.3.2.5 Luminescence lifetimes of the lanthanide emission

Luminescence lifetime measurements were performed to quantify how well the lanthanides are protected from non-radiative deactivation and how many species (with different coordination environment) are present in solutions. Results for Nd$_8$/PAMAM-1, Sm$_8$/PAMAM-1 and Eu$_8$/PAMAM-1 are collected in Table 3-20. Single exponential decays obtained by fitting of the decay curves with Origin software indicate presence of only one major species with the same coordination environment in the solution.

Table 3-20: Lifetimes of the metal centered luminescence of selected lanthanide complexes. T=298 K, λ_{ex} = 337.1 nm.

	Nd_8/PAMAM-1 (DMSO)	Sm_8/PAMAM-1 (DMSO)	Eu_8/PAMAM-1 (DMSO)
Ln^{3+} luminescence lifetime	1.77 µs +/- 0.01	20.00 µs +/- 0.01	1.10 ms +/-0.06

3.3.2.6 Singlet and triplet states in the Ln_8/PAMAM-1 complexes

Gadolinium and lanthanum are silent lanthanides in complexes. This is due to electronic energy levels that are too high in energy to be accessible (Gd) or to the absence of f-electrons (La). However, in complexes these lanthanides induce the same perturbation to the ligand as other lanthanides. The energy located on the triplet state energy level is not transferred to Gd or La, but is emitted as phosphorescence or lost by non-radiative deactivation. The triplet state (and singlet state) population is increased by lowering the temperature to 77 K, which decreases the efficiency of vibrational deactivation by OH, NH, CH or other oscillators (Chapter 1.1).[6] This facilitates an investigation of the position of the triplet state energy level (T_1) and triplet state luminescence lifetime.

Complexes of PAMAM-1 with Gd^{3+} and La^{3+} were prepared and their fluorescence and phosphorescence spectra were recorded. The fluorescence spectra are depicted in Figure 3-21 and Figure 3-22 and the phosphorescence spectra are depicted in Figure 3-19 and Figure 3-20. For experimental parameters see Chapter 3.2.6.

The luminescence lifetimes of the triplet states were measured. The locations of the singlet and triplets states were determined through the ligand fluorescence and phosphorescence spectra,

respectively. The luminescence lifetimes provide insight into the mechanism of energy transfer and quenching of the excited states of the Ln(III). The following results were obtained: Singlet State: (Gd_8/PAMAM-1) emission maximum is located at 375 nm (broad); (La_8/PAMAM-1) emission maximum is located at 375 nm (broad). Triplet state (Gd_8/PAMAM-1) emission maximum at 486 nm (20,576 cm^{-1}) assigned to 0,0 transition and maxima at 521 nm (19,193 cm^{-1}), 561 nm (17,825 cm^{-1}) and 608 nm (16,447 cm^{-1}) which are the vibronic progressions. The energy differences between the vibrational bands are in the range of ~1,376 cm^{-1}. Triplet state (La_8/PAMAM-1) emission maxima are located at 486 nm (20,576 cm^{-1}), 522 nm (19,157 cm^{-1}) and 554 nm (18,050 cm^{-1}).

Table 3-21: Positions of the ligands energy levels in the Gd_8/PAMAM-1 and La_8/PAMAM-1 complexes.

Positions of the ligand energy levels	Gd_8/PAMAM-1		La_8/PAMAM-1	
	Wavelength	Energy	Wavelength	Energy
S_1	375 nm	26,667 cm^{-1}	375 nm	26,667 cm^{-1}
T_1	486 nm	20,576 cm^{-1}	486 nm	20,576 cm^{-1}

Emission Spectra: La$_8$/PAMAM-1 at 77K
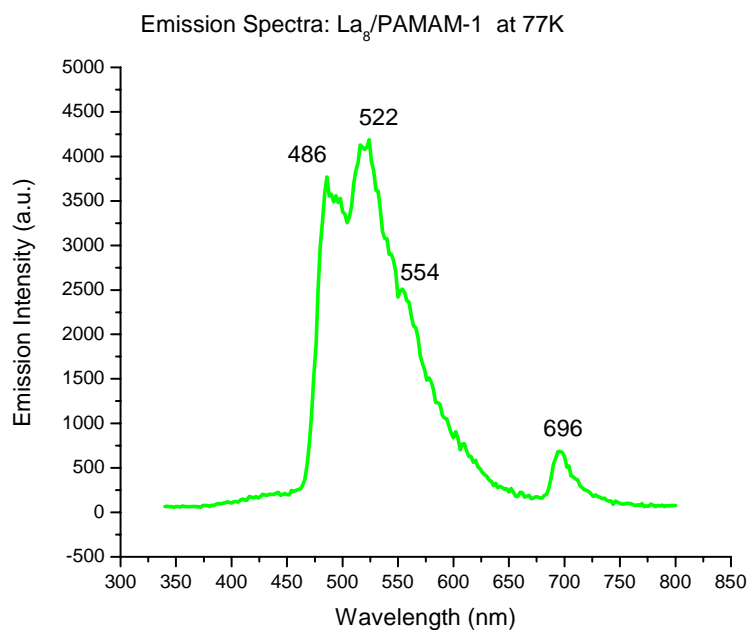
Figure 3-19: Phosphorescence spectrum of La$_8$/PAMAM-1. C=2.16x10^{-5} M. 77 K. λ_{ex}: 330 nm.

Gd$_8$/PAMAM-1, 77K, Emission Spectrum
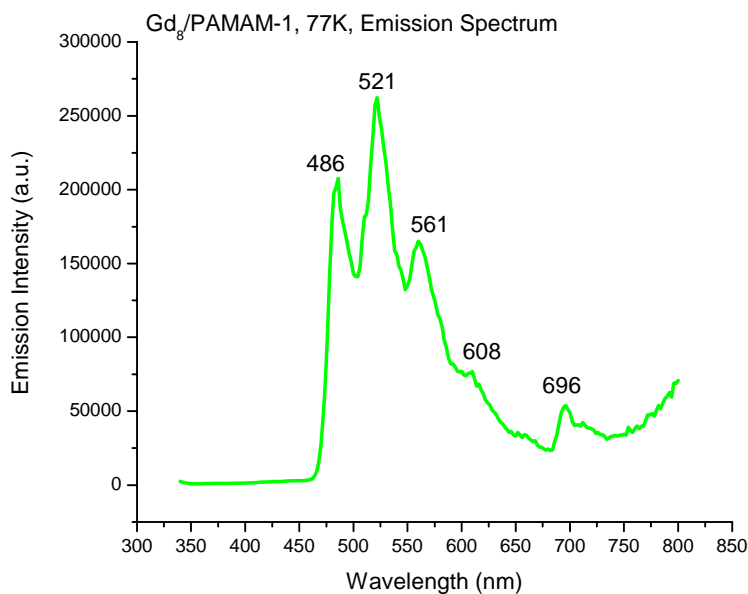
Figure 3-20: Phosphorescence spectrum of Gd$_8$/PAMAM-1. C=2.16x10^{-5} M. 77 K. λ_{ex}: 330 nm.

69
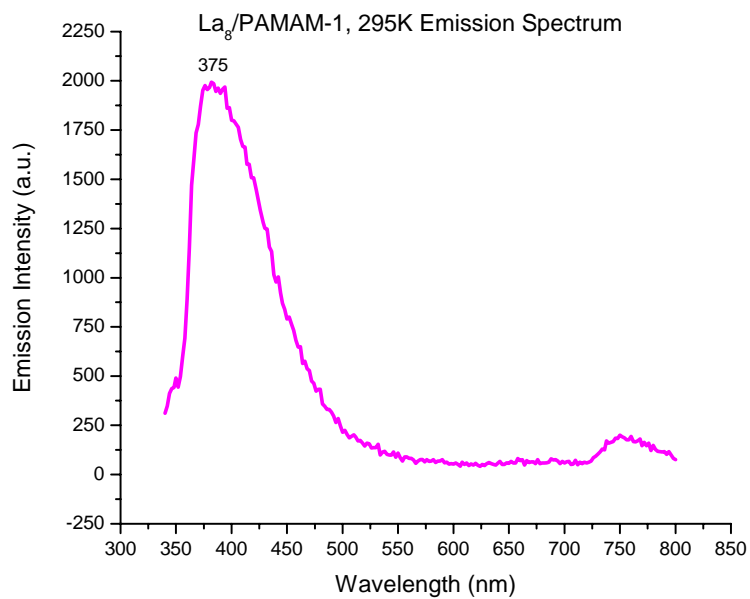
Figure 3-21: Fluorescence spectrum of La$_8$/PAMAM-1. C=2.16x10^{-5} M. 295 K. λ_{ex}: 330 nm.
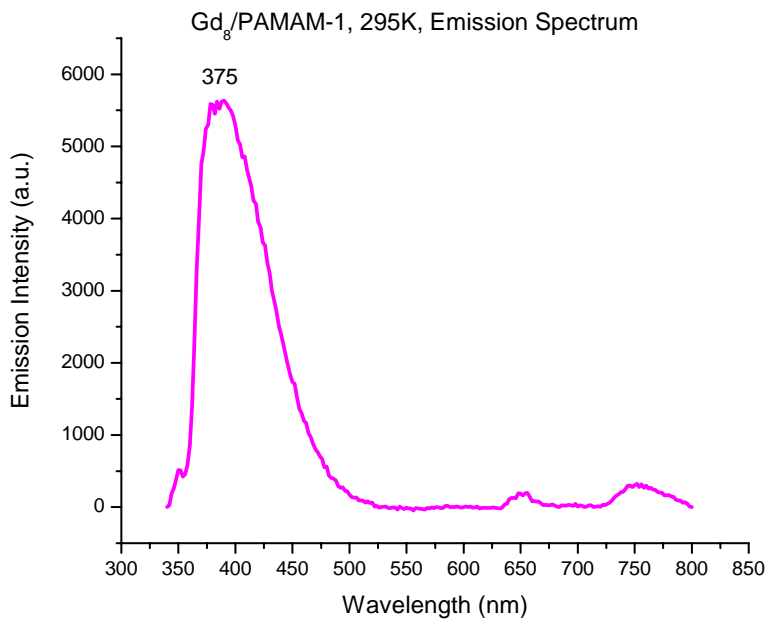
Figure 3-22: Fluorescence spectrum of Gd$_8$/PAMAM-1. C=2.16x10^{-5} M. 295 K. λ_{ex}: 330 nm.

Gd$_8$/PAMAM-1 Excitation and Emission Spectra
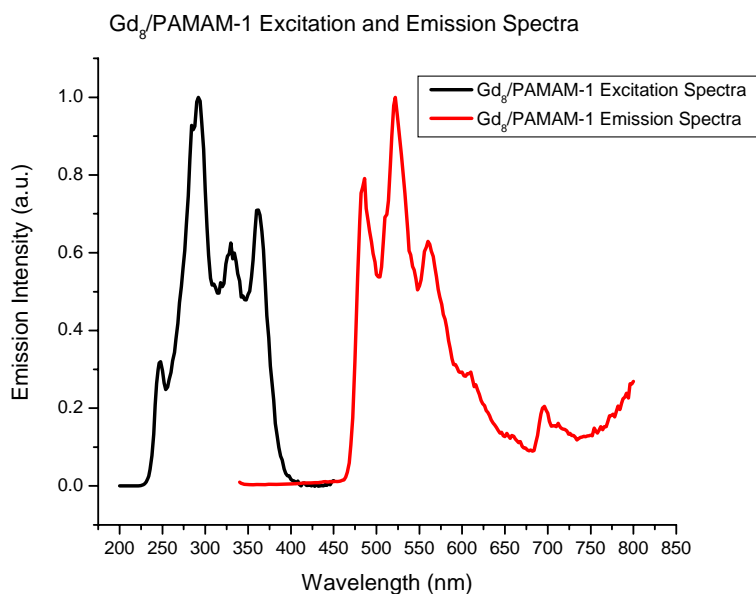
Figure 3-23: Time-resolved excitation and emission spectra of Gd$_8$/PAMAM-1. C=2.16x10-5 M. 77 K. λ_{ex} 330 nm. λ_{em} 486 nm.

Time-resolved emission spectra recorded at 77 K appear as one triplet state band structured by vibronic coupling; however, the luminescence lifetime measurements and fitting of the decay curve revealed presence of two distinctive luminescence lifetimes in each complex, which may indicate the presence of two independent triplet states. This hypothesis is in accordance with results obtained by other research group working on naphthalimides.[17] Luminescence lifetimes of the triplet states are summarized in Table 3-22.

Table 3-22: Luminescence lifetimes of the triplet states.

Luminescence lifetimes of the triplet states	Gd$_8$/PAMAM-1	La$_8$/PAMAM-1
t$_1$: $^3(n,\pi^*)$	0.16 +/- 0.01 s	0.36 +/- 0.07 ms
t$_2$: $^3(\pi,\pi^*)$	2.9 +/- 0.4 s	18 +/- 4 ms

Phosphorescence lifetimes may differ because they arise from different electronic states. Phosphorescence from a $^3(n,\pi^*)$ triplet is shorter lived (and more efficient if located at lower energy level) than a $^3(\pi,\pi^*)$ triplet because the transition to the S_0 ground state is somewhat more allowed as the result of mixing with the $^1(\pi,\pi^*)$ (spin-orbit interaction).[9, 28] However, according to the experimental results obtained by Cossanyi *et al*,[17] $^3(\pi,\pi^*)$ is the lower energy triplet state. Based on this information the t_1 lifetimes could be assigned to phosphorescence from the higher energy $^3(n,\pi^*)$ triplet state and the t_2 lifetimes to phosphorescence from the lower energy $^3(\pi,\pi^*)$ triplet state.

Triplet state luminescence lifetimes for the gadolinium complex are in range of seconds where as those for lanthanum complexes are in the millisecond range. These results are caused by the fact that Gd^{3+} ion has seven unpaired electrons, making it the most paramagnetic of all metal cations. Triplet states are also paramagnetic, so orbital spin interactions can occur and significantly increase the rate of intersystem crossing formation, which in turn increases the population of the triplet state. This is termed the heavy atom effect[4]. La^{3+} is diamagnetic since it has no unpaired electrons.
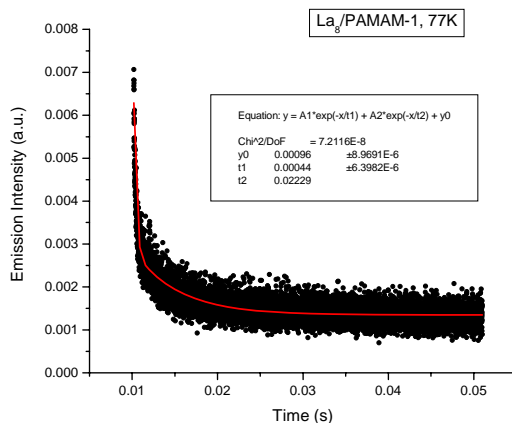
Figure 3-24: Example of fitted luminescence lifetime decay curve for La₈/PAMAM-1. C=2.16x10-5 M. 77K. Excitation wavelength: 337 nm.

72
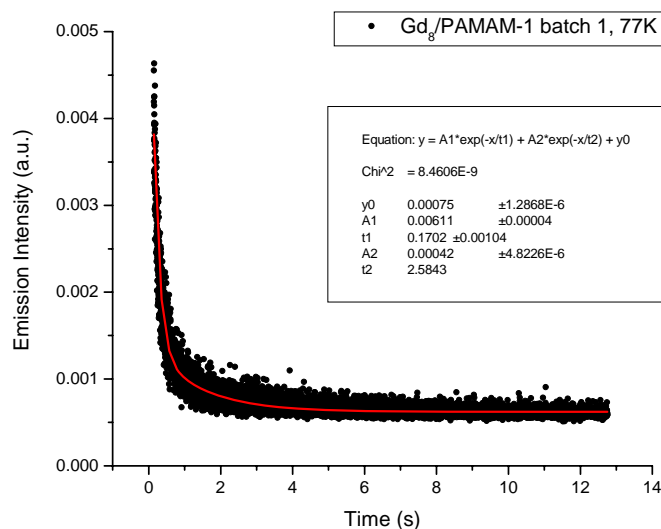
Figure 3-25: Example of fitted luminescence lifetime decay curve forGd$_8$/PAMAM-1. C=2.16x10-5 M. 77 K. Excitation wavelength: 337 nm.

3.3.3 Characterization of the species formed in solution and spectroscopic properties of the Ln/PAMAM-2 complexes

3.3.3.1 Batch luminescence spectrophotometric titrations

Spectrophotometric luminescence titration experiments performed with PAMAM-1 determined that this ligand forms complexes with the metal to ligand ratio of 1:7.5 in solution (Chapter 3.3.2). To verify that PAMAM-2 forms complexes with lanthanides in the same ratio, several batches of PAMAM-2 complexes in different ratios of Tb^{3+}, Eu^{3+}, and Nd^{3+} were prepared for batch spectroscopic luminescence titration as described in the experimental section (Chapter 2.2). The graphs showing the results of the spectroscopic titration are depicted in Figure 3-26 - Figure 3-28.
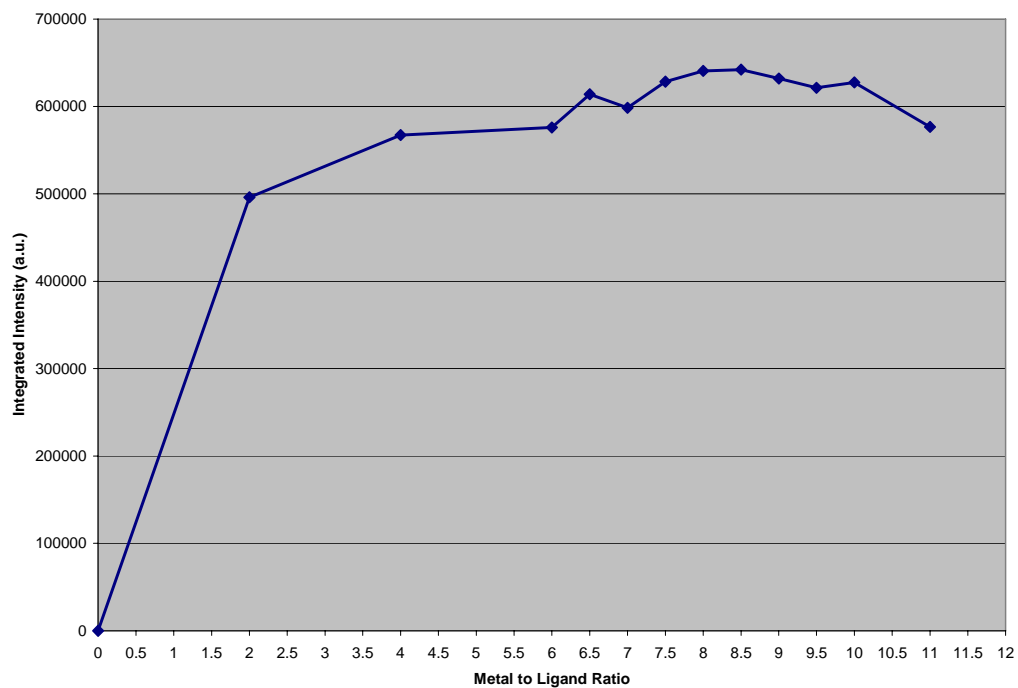
Figure 3-26: Plot of ratio of the metal ions to the ligand versus integrated intensity of Eu^{3+} emission.
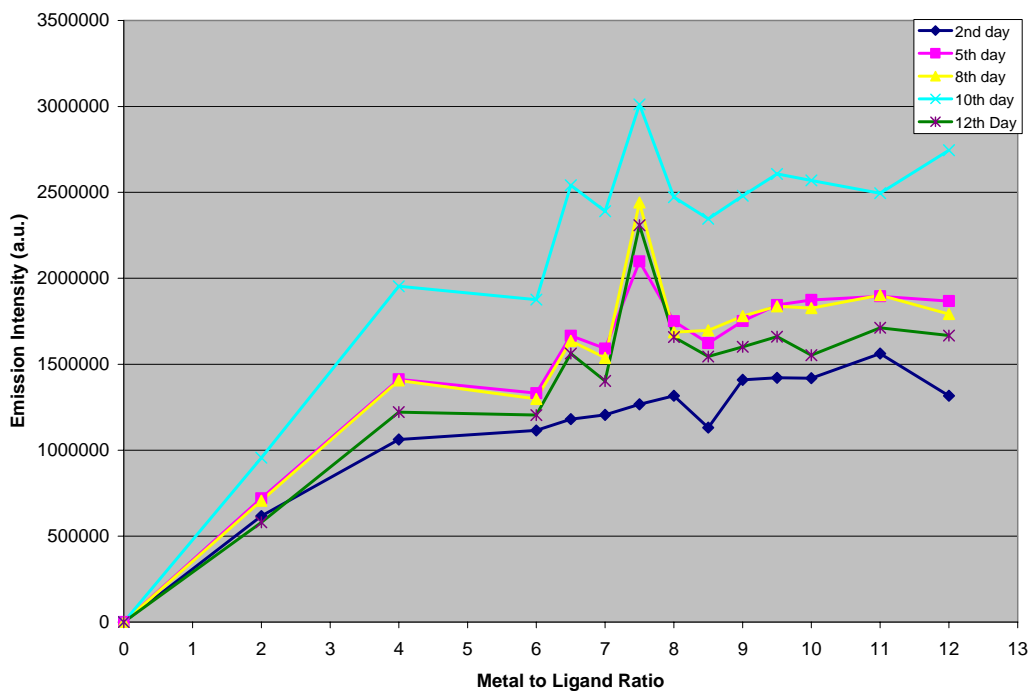
Figure 3-27: Plot of ratio of the metal ions to the ligand versus integrated intensity of Tb^{3+} emission.

74
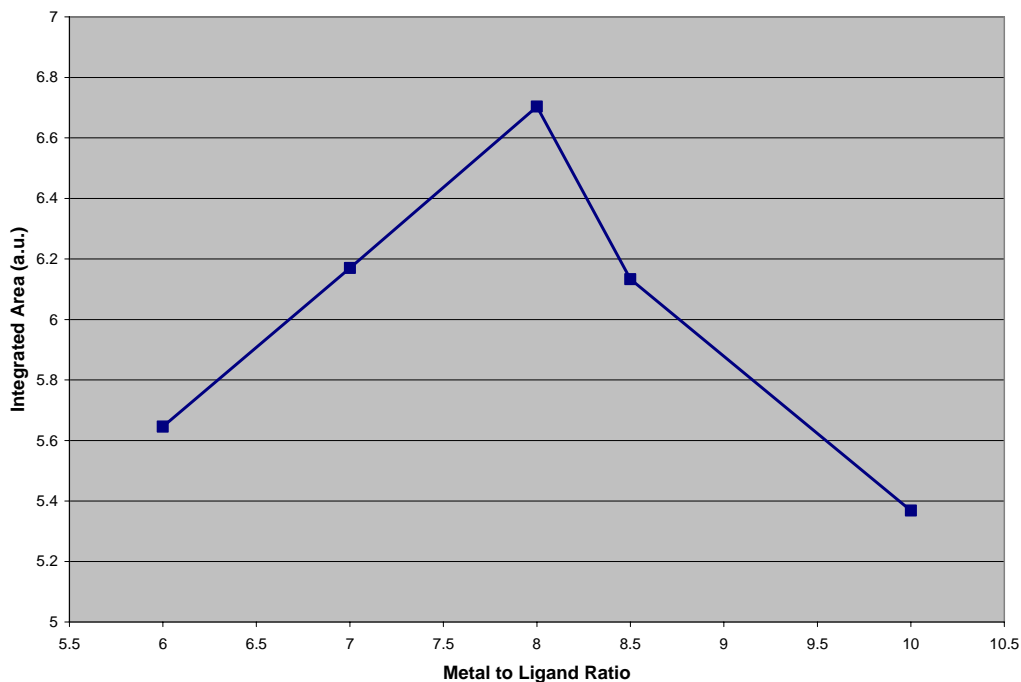
Figure 3-28: Plot of ratio of the metal ions to the ligand versus integrated intensity of Nd^{3+} emission.

The results obtained from the terbium titration reveal that PAMAM-2 forms complexes with Tb^{3+} ions with the most luminescent species at an average ratio of 7.5 (M:L). Titration of Eu^{3+} and Nd^{3+} show that the most luminescent species in solution are formed at the M:L ratio 8. The differences can be explained by the limit of accuracy of the measurements. Globally we can consider the average position of the breaking point to be eight, which would give the general formula for PAMAM-2 complexes with lanthanides Ln_8/PAMAM-2. Results obtained for PAMAM-2 are similar to these obtained for PAMAM-1, suggesting that both dendrimers form the same species in the solution.

3.3.3.2 UV/Vis absorption properties of the complexes

UV/Vis absorption spectra of several Ln_8/PAMAM-2 complexes (Ln = Eu, Gd, La) show no differences in the positions maxima of the absorption bands compared to free PAMAM-2 (Figure 3-29). The Ln_8/PAMAM-2 have one low absorption band at 286 nm, one band with strong absorption centered at 335 nm with shoulders at both lower and higher energy and one band with low absorption around 412 nm. The extinction coefficients differ between the free dendrimer and its lanthanide complexes (Table 3-23).

Table 3-23: Extinction coefficients (ε) for Ln_8/PAMAM-2 complexes

	Extinction coefficients $\varepsilon/dm^3 mol^{-1} cm^{-1}$		
	at 286 nm	at 335 nm	at 412 nm
PAMAM-2	132,530	288,530	2,483
Eu_8/PAMAM-2	360,200	731,560	10,743
Gd_8/PAMAM-2	329,990	656,490	4,742
La_8/PAMAM-2	336,660	593,250	4,995

The extinction coefficients (ε) are relatively large in comparison to organic molecules[27] except for the absorption band at 412 nm. As for PAMAM-1, this can be explained by the presence of 32 chromophoric groups in a discrete molecule. It is surprising that the band at 412 nm with the smallest value of ε is involved in the most efficient (vide infra) energy conversion to the accepting energy level of neodymium.
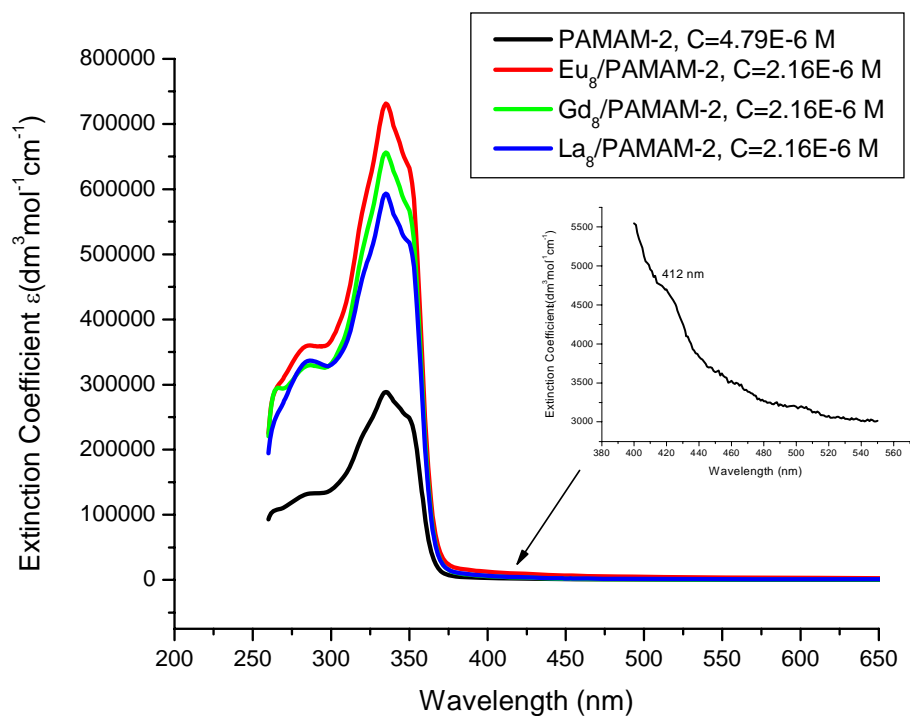
Figure 3-29: UV/Vis absorption spectra of PAMAM-2 and selected Ln$_8$/PAMAM-2 solutions in anhydrous DMSO at 295 K

3.3.3.3 Excitation and Emission spectra

PAMAM-2 can sensitize several lanthanide cations emitting in visible and NIR. Excitation and emission spectra obtained for Nd$_8$/PAMAM-2, Eu$_8$/PAMAM-2, and Tb$_8$/PAMAM-2 are depicted in Figure 3-30 through Figure 3-36.
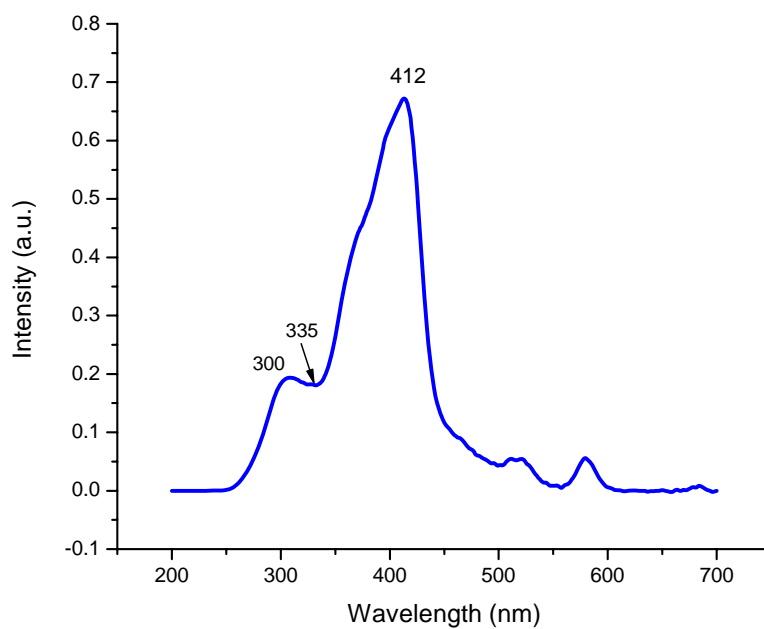
Figure 3-30: Excitation spectrum of Nd$_8$/PAMAM-2 complex, C=3.27E-6, λ_{em} 1060 nm
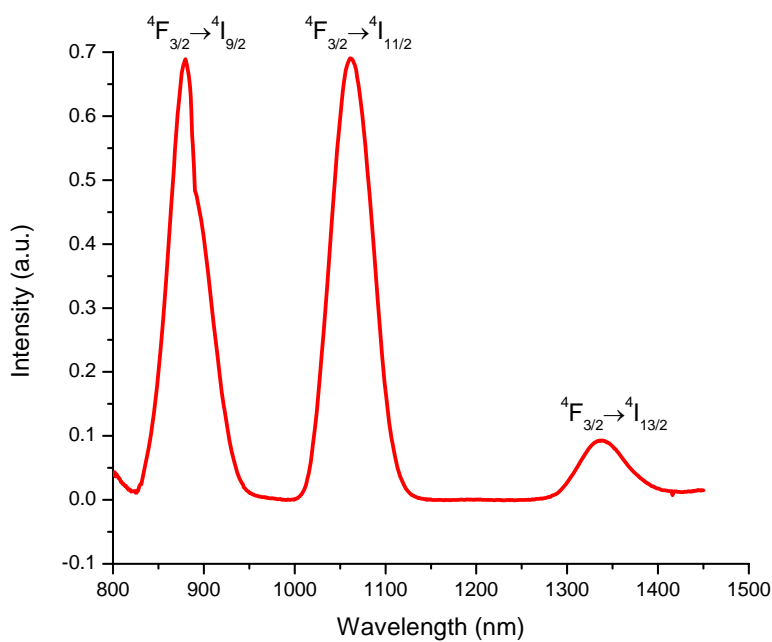
Figure 3-31: Emission spectrum of Nd$_8$/PAMAM-2 complex, C=3.27E-6, λ_{ex} 412 nm.

It can be observed in Figure 3-30 that the most efficient luminescence from neodymium in Nd$_8$/PAMAM-2 is obtained with 412 nm excitation, which corresponds to the absorption band with a relatively small extinction coefficient (this band appears as a small shoulder, Figure 3-29). This absorption band is more efficient in sensitizing neodymium than the band with the largest extinction coefficient centered at 335 nm. As a consequence, two different quantum yield values are expected for excitation wavelengths of 335 nm and 412 nm. Luminescence intensity is proportional to the extinction coefficient, to QY, and to the number of luminescent lanthanide cations. Since the ε value is low at 412 nm, significantly higher value of QY is expected.

Interestingly the opposite relation is observed for the europium complex Eu$_8$/PAMAM-2. Here the most intense Eu^{3+} luminescence arises from excitation at about 310 nm (Figure 3-32). This observation indicates different pathways of the sensitization energy. One possible explanation is that the sensitization of europium and neodymium occurs from two different triplet states located at different energy levels. The accepting energy level of europium is higher in energy than the accepting energy level of neodymium (see Figure 1-7). Measurements of the position of the singlet and triplet states need to be done to verify this hypothesis.
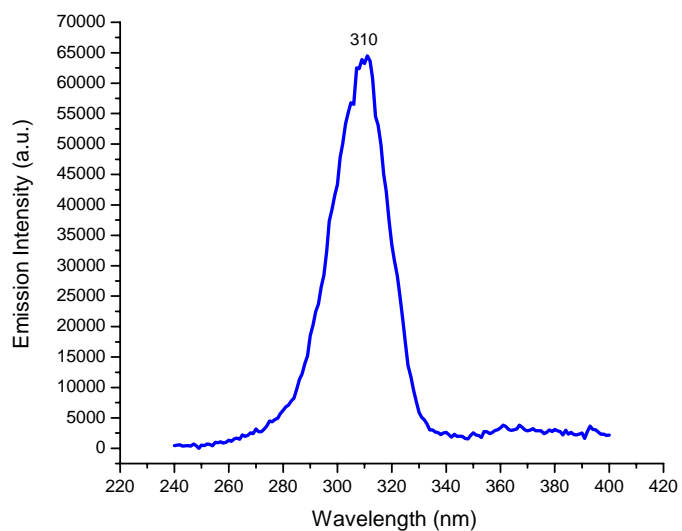
Figure 3-32: Excitation spectrum of Eu$_8$/PAMAM-2 complex, C=2.16E-6, λ_{em} 615 nm
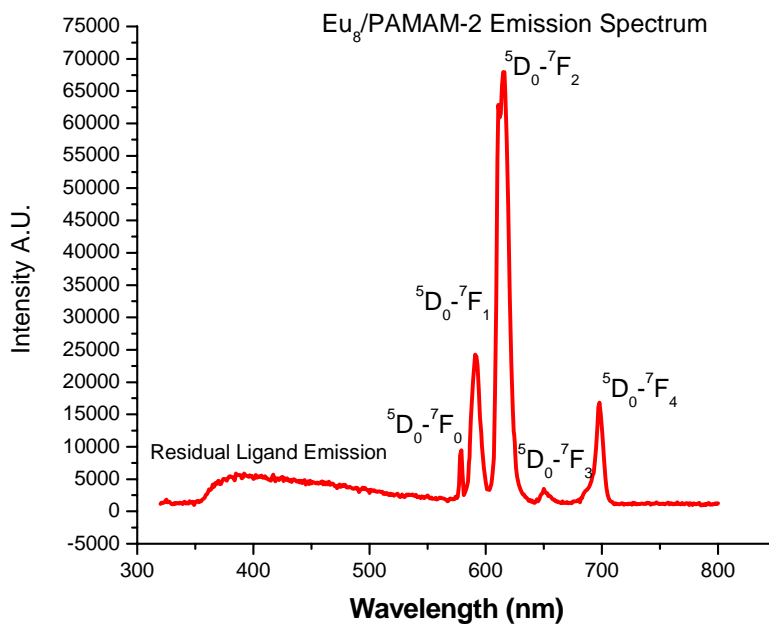
Figure 3-33: Emission spectrum of Eu$_8$/PAMAM-2 complex, C=2.16E-6, λ_{ex} 300 nm.
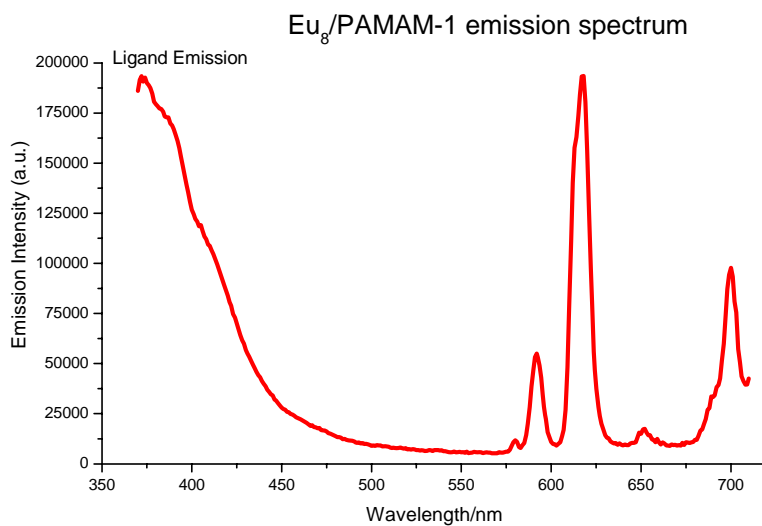
Figure 3-34: Emission spectrum of Eu$_8$/PAMAM-1 complex presented here for comparison. λ_{ex} 360 nm
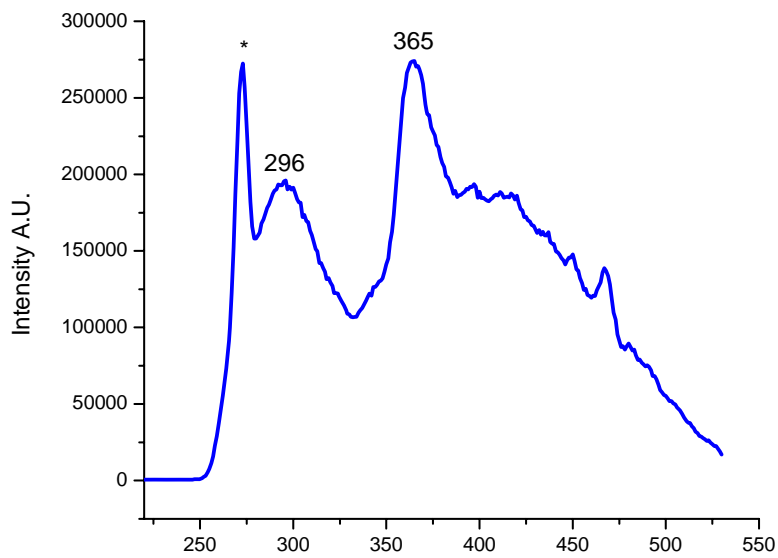
Figure 3-35: Excitation spectrum of Tb$_8$/PAMAM-2 complex, C=2.16E-6, λ_{em} 543 nm. "*" indicate artifact generated by the grating.
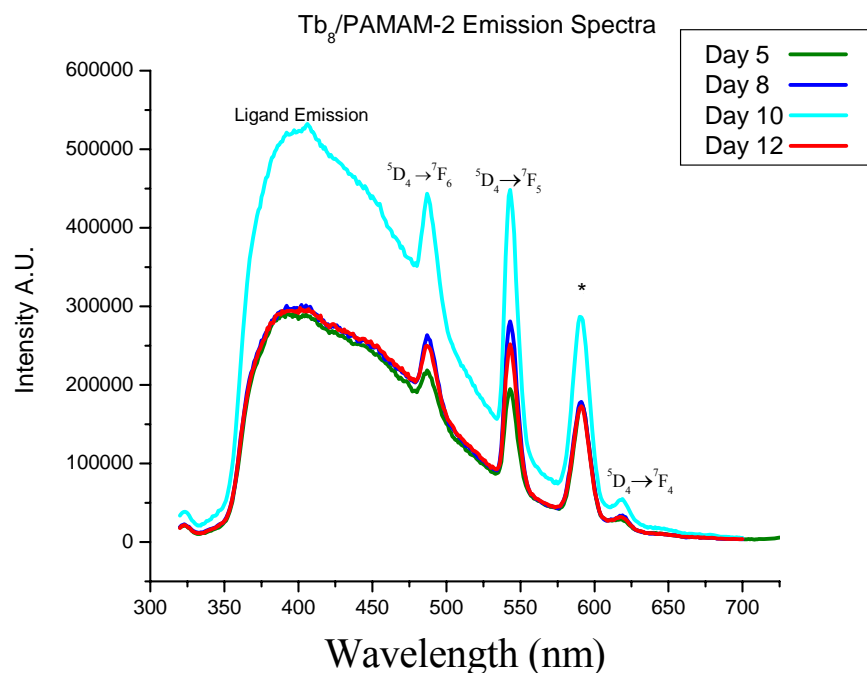
Figure 3-36: Emission spectrum of Tb$_8$/PAMAM-2 complex, C=2.16E-6, λ_{ex} 296 nm. "*" indicate 2nd order signal generated by the grating.

The comparison of Eu$_8$/PAMAM-2 and Tb$_8$/PAMAM-2 emission spectra (Figure 3-33 and Figure 3-36) is also interesting. The ligand emission band is significantly smaller for the europium complex, which indicates more efficient energy transfer from the ligand to Eu^{3+}.

3.3.3.4 Luminescence lifetimes of the lanthanide emission

Luminescence lifetime measurements were performed to quantify how well the lanthanides are protected from non-radiative vibrational deactivations and how many species (with different coordination environment) are present in solution. Comparing the results for neodymium and europium complexes with PAMAM-1 and PAMAM-2 shows the lanthanide cations may have

the same level of protection in both dendrimers. This assumption is based on the hypothesis that coordination geometries in both complexes are similar. Single exponential decay curves for each complex indicate the presence of only one major species with the same or close coordination environment in solution. The results are summarized in the Table 3-24:

Table 3-24: Lifetimes of the metal centered luminescence of selected lanthanide complexes. T=298 K, λ_{ex} = 337.1 nm.

	Nd$_8$/PAMAM-2 (DMSO)	Tb$_8$/PAMAM-2 (DMSO)	Eu$_8$/PAMAM-2 (DMSO)
Ln^{3+} luminescence lifetime	1.53 µs +/- 0.02	1.8 ms +/-0.7	1.33 ms +/-0.01

3.3.3.5 Quantum Yields

As predicted, QY measurement for Nd$_8$/PAMAM-2 solution in DMSO gave different values for excitation wavelengths at 330 – 360 nm and 445 nm, with the higher QY value obtained for the later. The difference is in the order of 10^2. Quantum yields values for Nd$_8$/PAMAM-2, Tb$_8$/PAMAM-2 and Eu$_8$/PAMAM-2 complexes in DMSO are summarized in Table 3-25.

Table 3-25: Quantum yields of selected Ln$_8$/PAMAM-2 complexes in anhydrous DMSO.

	Quantum Yield		
	330 nm	360 nm	445 nm
Nd$_8$/PAMAM-2	7.2 +/- 0.3 x 10^{-6}	9.9 +/- 0.4 x 10^{-6}	4.3 +/- 0.2 x 10^{-4}
Tb$_8$/PAMAM-2	_____	1.1 +/- 0.4 x 10^{-4}	_____
Eu$_8$/PAMAM-2	_____	0.019 +/- 0.005	_____

This data shows that the most efficient energy transfer and sensitization occurs for Eu$_8$/PAMAM-2 complexes and the least efficient for Nd$_8$/PAMAM-2. The positions of the donating energy levels of the sensitizer and accepting levels of the lanthanides can tentatively explain this. The more ideal the match in energy levels between the ligand and sensitizer, the better the energy transfer, as in the case of Eu^{3+} and PAMAM-2. The accepting energy level of Tb^{3+} is located about 420 cm^{-1} above the donating triplet state energy level of the sensitizer. Such situation is not favorable for energy transfer, lowering the quantum yield.

Quantum yields for NIR emitting neodymium complexes compared with visible emitting lanthanides are generally lower. This is due the excited state energy level of neodymium being relatively low and much closer to the ground state than it is in the lanthanides emitting in visible, such as europium or terbium. Therefore, the neodymium excited state is more easily deactivated by vibrations of suitable energies.

The values obtained for Tb$_8$/PAMAM-2 complex is relatively low in comparison to QY reported for other Tb^{3+} complex, which is as high as 60%[10]. The QY for a Nd/tropolone complex synthesized in our group is 0.2%,[11] which is about 200 times greater than the QY for Nd$_8$/PAMAM-2. Nevertheless, the emission from PAMAM-2 complexes is intense, due to the high number of chromophoric groups and lanthanide ions in the dendrimer complex. It is especially noticeable for Nd$_8$/PAMAM-2 complex, which has the lowest quantum yield but emits NIR radiation intense enough to be detected in the living cell (further discussed in Chapter 3.3.4).

3.3.3.6 Singlet and triplet states in the Ln$_8$/PAMAM-2 complexes

Gd$_8$/PAMAM-2 was prepared and fluorescence and phosphorescence spectra were recorded to locate the singlet and triplet state energy level positions. The phosphorescence spectra obtained with time-resolved measurements are depicted in Figure 3-37 and Figure 3-38. For experimental parameters see Chapter 3.2.9.3.
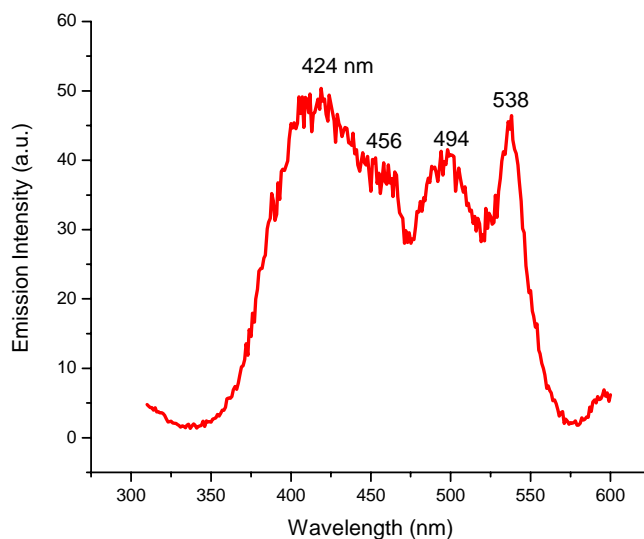
Figure 3-37: Phosphorescence emission spectrum of Gd$_8$/PAMAM-2 (T$_1$). C=2.16x10^{-5} M. 77 K. λ_{ex}: 300 nm, λ_{ex}: 424 nm.
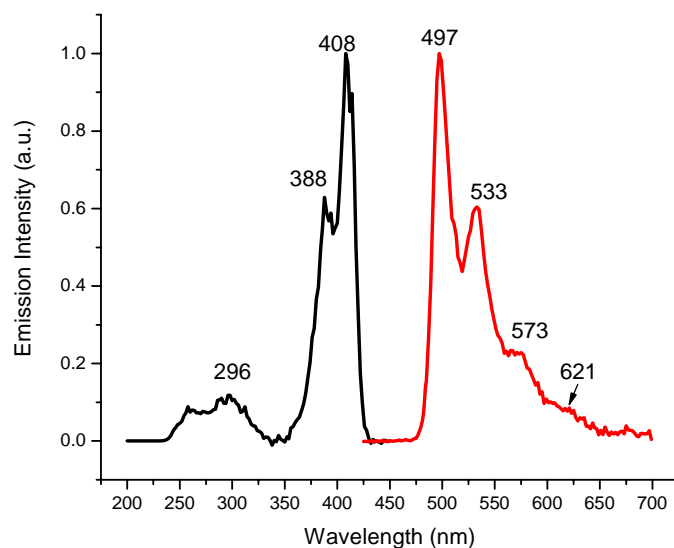
Figure 3-38: Phosphorescence excitation and emission spectra of Gd$_8$/PAMAM-2 (T$_2$). C=2.16x10^{-5} M. 77 K. λ_{ex}: 408 nm, λ_{ex}: 497 nm.

The following results have been obtained: singlet state emission maxima: (S$_1$) 375nm (26,667 cm^{-1}) and (S$_2$) 475 nm (21,053 cm^{-1}). Triplet state emission maxima: (T$_1$) 424 nm (23,585 cm^{-1}) assigned to the 0,0 transition with three bands which are the vibronic progressions 456 nm (21,930 cm^{-1}), 494 nm (20,243 cm^{-1}) and 538 nm (18,587 cm^{-1}), (T$_2$) 497 nm (20,121 cm^{-1}) assigned to the 0,0 transition with vibronic progressions 533 nm (18,762 cm^{-1}), 573 nm (17,452 cm^{-1}) and 621 nm (16,103 cm^{-1}). The energy differences between the vibrational bands are in the range of ~ 1,665 cm^{-1} (T$_1$) and ~ 1,340 cm^{-1} (T$_2$). Positions of the singlet and triplet states are summarized in the Table 3-26. As expected, based on the results obtained by other research groups working on naphthalimides,[17] the presence of two independent triplet states was found. Luminescence lifetimes measurements of the phosphorescence will quantify these energy levels.

Table 3-26: Positions of the ligands energy levels in the Gd$_8$/PAMAM-2 complex.

Positions of the ligand energy levels	Gd$_8$/PAMAM-2	
	Wavelength	Energy
S$_1$	375 nm	26,667 cm^{-1}
S$_2$	475 nm	21,053 cm^{-1}
T$_1$	424 nm	23,585 cm^{-1}
T$_2$	497 nm	20,121 cm^{-1}

3.3.4   Application of the complexes for NIR bio-imaging and oxygen sensing in vivo

One of the fundamental goals of this project is the application of polymetallic dendrimer complexes in bioimaging and oxygen sensing in the living cell. Using the complexes developed here, NIR emission of the Nd dendrimer complex was observed for the first time in fluorescent microscopy (Figure 3-39).
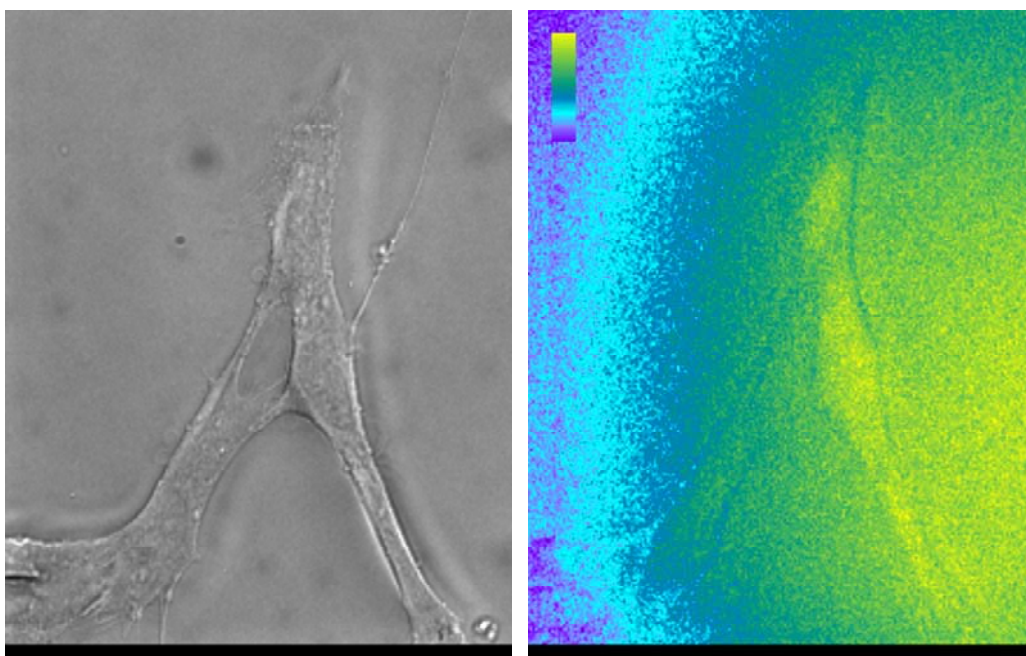
Figure 3-39: The traditional (left side) and NIR imaging (right side) of the living cell.

In order to test the luminescence intensity and stability of the complex for *in vivo* experimental conditions, and to monitor the ability of Nd_8/PAMAM-2 to sense oxygen in these conditions, the complex was tested in living cells through our existing collaboration with Professor Claudette M. St Croix (Department of Environmental and Occupational Health, University of Pittsburgh) and Professor Simon C. Watkins (Director of the center for Biological Imaging of the University of Pittsburgh. The complex was micro-injected as a concentrated DMSO solution in a living rat lung endothelial cell. Oxygen concentration was varied during the experiment from 1.5% to 60%. The results (reported below in Figure 3-40) indicate that the luminescent lanthanide complex can be detected with a good sensitivity in fluorescence microscopy: the decrease of oxygen concentration from 21% to 1.5% induced an increase of the luminescence signal of 60%. This preliminary experiment is the first example of a luminescent lanthanide complex emitting in

the near-infrared domain used for fluorescence microscopy in cell. It demonstrates that the complex used is luminescent and stable enough to be used as a reporter in physiological conditions. The ability of the complex to be used as oxygen sensor in a favorable dynamic range was also demonstrated since hypoxia caused a 60% increase in emission intensity.
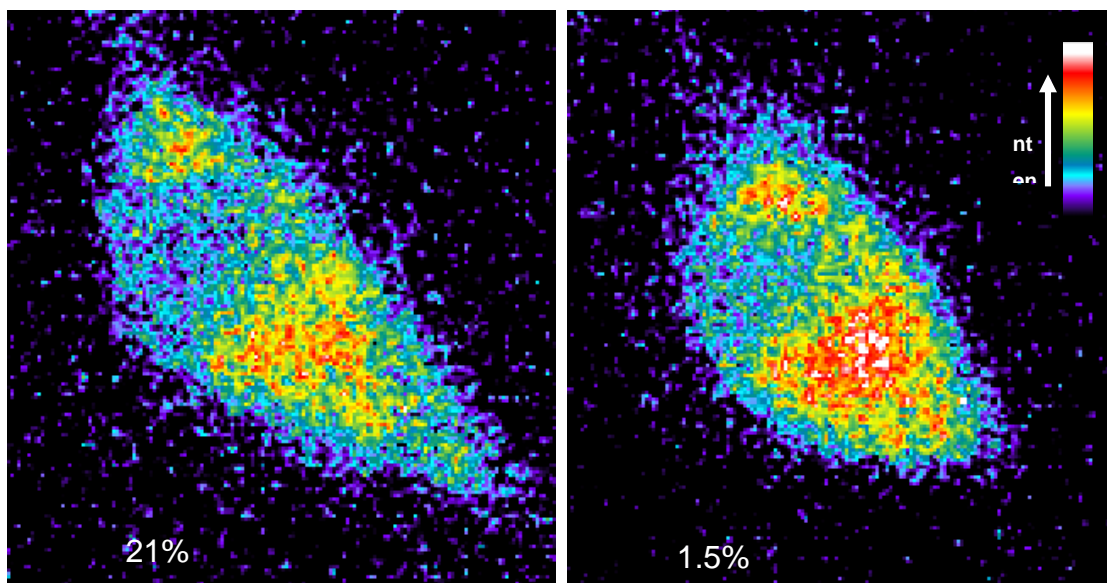
Figure 3-40: Real time imaging of the NIR emitting and O$_2$-sensitive complex Nd$_8$/PAMAM-2 microinjected into a rat lung endothelial cell. 21% and 1.5% - concentration of oxygen, λ_{ex} = 380 nm.

3.3.5   Comparison of the properties of PAMAM-1 and PAMAM-2

Batch spectrophotometric titrations revealed that both PAMAM dendrimer ligands studied here form complexes with lanthanide ions in ratios of 1:7.5–1:8; thus, the general formula Ln$_8$/PAMAM was used. The dendrimer lanthanide complexes have a slow kinetic of formation, requiring one week to form the most luminescent species in solution.

Absorption bands of the free ligands and their complexes are in the same energy positions, indicating that the Ln^{3+} ions coordinate to the interior branches of the dendritic ligands, most likely to the amide's oxygen atoms.

PAMAM-1 and PAMAM-2 demonstrated the ability to sensitize visible and NIR emitting lanthanides cations. PAMAM-2 complexes were synthesized with Eu^{3+}, Tb^{3+}, and Nd^{3+} and analyzed. Comparison of the emission spectra of Eu_8/PAMAM-1 and Eu_8/PAMAM-2 reveal more efficient energy transfer for PAMAM-2. The emission band assigned to the ligand is significantly less intense in the case of PAMAM-2 relative to the europium emission band (compare Figure 3-33 and Figure 3-34). Quantum yield measurements confirm this trend (6.0×10^{-4} for Eu_8/PAMAM-1 vs. 1.9×10^{-2} for Eu_8/PAMAM-2). Another comparison between Tb_8/PAMAM-2 and Eu_8/PAMAM-2 (Figure 3-33 and Figure 3-36) illustrates that Eu^{3+} is better sensitized than Tb^{3+} (confirmed by QY values: 1.06×10^{-4} for Tb_8/PAMAM-2 vs. 1.9×10^{-2} for Eu_8/PAMAM-2). Quantum yield measurements show also that neodymium is sensitized by PAMAM-2 with the lowest efficiency (9.86×10^{-6}); however, QY for neodymium complexes are generally lower, as explained earlier in Chapter 3.3.3.5. Nevertheless the high number of chromophores (32) and coordinated Ln^{3+} (8) for each discrete dendrimer complex assure intense luminescence.

Based on the excitation and absorption spectra it can be hypothesized that neodymium and europium in the PAMAM-2 complexes are sensitized from different ligand energy levels (Figure 3-30 Figure 3-32). The excitation maxima for both complexes are located in different energy positions. It is not the case for PAMAM-1 complexes with neodymium and europium, where both complexes have the same excitation band centered at 330 nm (Figure 3-16 and Figure 3-17). The positions of the donating energy levels of the sensitizers and accepting levels of the

lanthanides cause these differences. A diagram illustrating the positions of energy levels for selected lanthanides and both dendrimers is depicted in Figure 3-41.
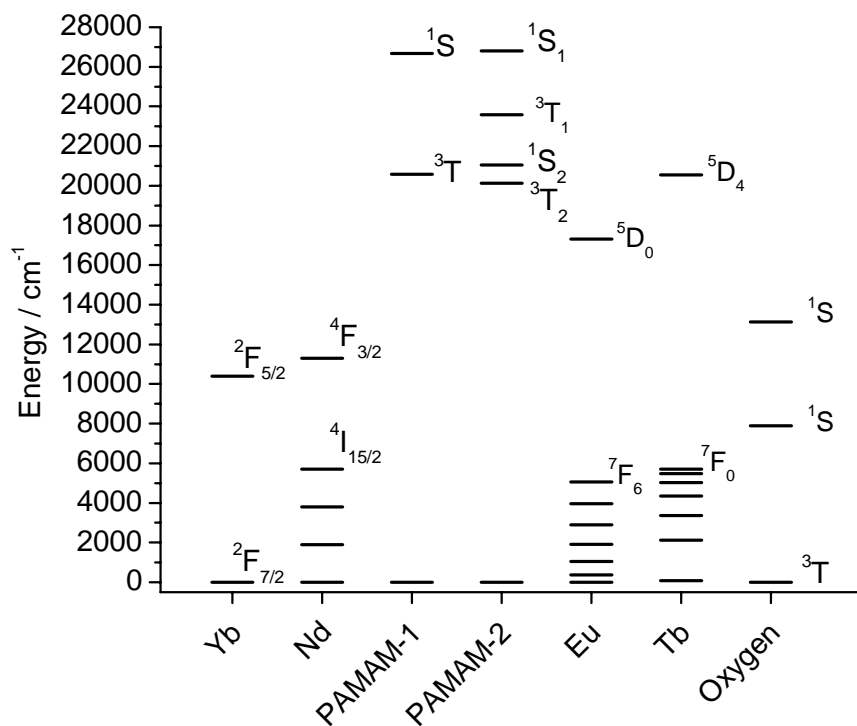
Figure 3-41: Some energy levels of selected lanthanides and PAMAM-1 and PAMAM-2 ligands.

Luminescence lifetime measurements revealed that both PAMAM-1 and PAMAM-2 may provide the same level of protection for bound lanthanide ions from deactivation by solvent molecules. Single exponential decays indicate that for each complex in solution there is one major species with a well defined environment. The luminescence lifetimes and quantum yields are summarized in Table 3-27. Single exponential decays indicate that for each complex in solution there is one major species with a well defined environment. The luminescence lifetimes and quantum yields are summarized in Table 3-27.:

Table 3-27: Quantitative data for selected Ln_8/PAMAM-1 and Ln_8/PAMAM-2 complexes (at 298 K).

Lanthanide ion	Ln_8/PAMAM-1 [DMSO]		Ln_8/PAMAM-2 [DMSO]	
	Quantum Yield	**Lumin. lifetime**	**Quantum Yield**	**Lumin. lifetime**
Eu^{3+}	6.0×10^{-4} +/-0.9×10^{-4}	1.10 ms +/-0.06	1.9×10^{-2} +/- 0.5×10^{-2}	1.33 ms +/-0.01
Tb^{3+}	‒‒‒	‒‒‒	1.1×10^{-4} +/- 0.4×10^{-4}	1.8 ms +/-0.7
Sm^{3+}	‒‒‒	20.00 μs +/-0.01	‒‒‒	‒‒‒
Nd^{3+}	‒‒‒	1.77 μs +/- 0.01	9.9×10^{-6} +/- 0.4×10^{-6}	1.53 μs +/- 0.02

3.4 CONCLUSIONS

The concept of polymetallic lanthanides – PAMAM dendrimer complexes with two different naphthalimides as sensitizers has been tested. In opposite to the classical approach where Ln^{3+} cation is bond by several ligands, in this system one branched ligand is bound to several lanthanides. This design allows the covalent attachment of 32 chromophore groups acting as antennae. The high absorption extinction coefficients of such modified dendrimer molecules allow them to absorb a large amount of energy for sensitizing coordinated lanthanide ions. The dendrimers also protect lanthanide ions from non-radiative deactivation from solvent molecules.

The chromophores demonstrate versatile sensitization of different lanthanide cations emitting in visible and NIR domains. Few chromophores are able to sensitize NIR emitting lanthanides because of the ease of their non-radiative deactivation.

The Nd_8/PAMAM-2 complex, regardless of its relatively low quantum yield, exhibited relatively intense luminescence and was successfully applied in a biological system. Not only was neodymium luminescence detected with fluorescence microscope (equipped with NIR sensitive camera) inside of the living cell for the first time, but this complex was also able to sense the changes in the oxygen concentration in the living cell *in vitro*. These results obtained with a lanthanide complex emitting in the NIR range demonstrate the vast potential for lanthanide complexes made with this family of dendritic ligands and open access to wide applications in the biology and medicine.

3.5 FUTURE WORK

The future work will be continued in several directions. First of all higher generations (G4 - G8) of this family of dendrimers will be synthesized and complexes with lanthanides prepared in order to investigate and analyze their photophysical properties. The structure of the PAMAM-1 molecule was simulated through MM3 molecular mechanics calculations (CaChe Workstation Pro 6.1.10, Fujitsu Ltd, USA). Solvent interactions were not taken into account. The result as a space filling structure is shown in Figure 3-42.
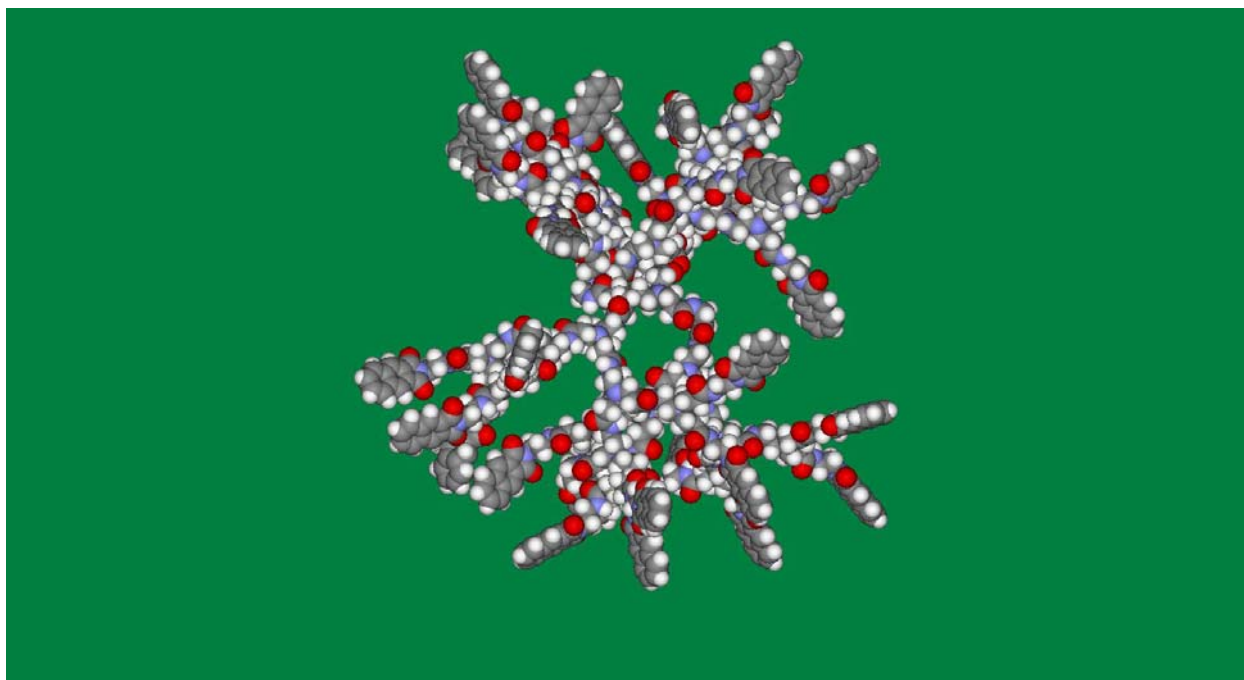
Figure 3-42: CaChe molecular modeling simulation for PAMAM-1 dendrimer.

As it can be seen the dendrimer possesses significant remaining space between the arms; therefore, it is worth increasing the generation of this family of dendrimers in order to increase

the overall luminescence intensity by incorporating larger numbers of lanthanide cations and chromophoric groups. This analysis will provide information on the maximum number of lanthanide cations that can be incorporated into such dendrimer species in order to maximize the luminescence intensity. We will examine how the kinetic and thermodynamic properties of the resulting lanthanide complexes are correlated to the size of the dendrimer ligand. By varying the size of the dendrimer ligands, it will be possible to determine if the photophysical properties of the dendrimer are directly proportional to the generation of the dendrimer and what the size limit is. Predictions of the spectroscopic properties of several generations of dendrimer complexes with lanthanide ions were made based on the preliminary results obtained in our group.[25] The experimental and predicted results are summarized in Table 3-28.

Table 3-28: Prediction of the luminescence efficiency based on the generation of the PAMAM dendrimer.

Dendrimer generation	Approxi-mate diameter of the dendrimer [nm][a]	Number of chromophores	Number of amide oxygens	Quantum yield %	$\varepsilon(360nm)$ [M^{-1}cm^{-1}]	Number of lanthanide cations per ligand	Lumines-cence efficiency[d]
3	>3.6	32	60	0.06[b]	74,473[b]	8.0[b]	**35,747**
4	>4.5	64	124	0.06[c]	148,946[c]	16.5[c]	**147,457**
5	>5.4	128	252	0.06[c]	297,892[c]	33.6[c]	**600,550**
6	>6.7	256	508	0.06[c]	595,784[c]	67.7[c]	**2,420,075**
7	>8.1	512	1,020	0.06[c]	1,191,568[c]	136.5[c]	**9,758,942**
8	>9.5	1,024	2,044	0.06[c]	2,383,136[c]	272.5[c]	**38,964,274**

[a] Values from the reference[15]
[b] Experimental values from the reference[25]
[c] Predicted by extrapolation of results obtained from the generation 3 dendrimer
[d] The luminescence efficiency is defined by the product of the absorbance by the number of lanthanide cations by the quantum yield.

The number of chromophores, amide's oxygen atoms and tertiary amines in the family of PAMAM dendrimers can be calculated from the following formulas: 2^{n+2} (number of chromophores), $2^{n+3} - 4$ (number of oxygen atoms) and $2^{n+2} - 2$ (number of tertiary amines).

Secondly, we will synthesize PAMAM-3 - dendrimers with 1,2- naphthalimides on the surface as a sensitizer which has been proposed in Table 1-1. The photophysical properties of the prepared complexes with lanthanides will be analyzed and compared with these of PAMAM-1 and PAMAM-2. This will allow us to rationalize how the photophysical properties of lanthanide complexes are affected by the electronic structure of the chromophoric groups. Among the proposed analysis, we will measure the phosphorescence lifetimes of the different naphthalimide triplet states in complexes with silent lanthanides (Gd^{3+}) and luminescent lanthanides (Eu^{3+}, Nd^{3+}). These measurements will allow obtaining the rate of energy transfer. This experiment should be possible since the triplet states of naphthalimide derivatives are highly populated and the ligands to lanthanide energy transfers are not complete.

If required we will modify the surface of the dendrimers to improve the water solubility and better compatibility with the biological systems. Presence of the primary amine groups to each naphthalimide on the surface of the dendrimer will make them water soluble and enable them to enter the cell.[29] This can be achieved by using the dendrimer 4-nitro-naphthalimides as a starting material for modification instead of naphthalimides. Reduction of the nitro groups to primary amines will lead to the proposed improvement.

BIBLIOGRAPHY

1.   Sabbatini, N.; Guardigli, M.; Lehn, J. M., Luminescent Lanthanide Complexes as Photochemical Supramolecular Devices. Coordination Chemistry Reviews 1993, 123, (1-2), 201-228.

2.   Atkins, P.; Paula, J. d., Physical Chemistry. 7th. ed.; Oxford University Press.

3.   Ceroni, P.; Bergamini, G.; Marchioni, F.; Balzani, V., Luminescence as a tool to investigate dendrimer properties. Progress in Polymer Science 2005, 30, (3-4), 453-473.

4.   Skoog, D., A.;; Holler F., J.; Nieman, T., A., Principles of Instrumental Analysis. 5th. ed.; Harcourt Brace & Company: Philadelphia, 1998.

5.   Silva, F. R. G. E.; Malta, O. L.; Reinhard, C.; Gudel, H. U.; Piguet, C.; Moser, J. E.; Bunzli, J. C. G., Visible and near-infrared luminescence of lanthanide-containing dimetallic triple-stranded helicates: Energy transfer mechanisms in the Sm-III and Yb-III molecular edifices. Journal of Physical Chemistry A 2002, 106, (9), 1670-1677.

6.   Beeby, A.; Clarkson, I. M.; Dickins, R. S.; Faulkner, S.; Parker, D.; Royle, L.; de Sousa, A. S.; Williams, J. A. G.; Woods, M., Non-radiative deactivation of the excited states of europium, terbium and ytterbium complexes by proximate energy-matched OH, NH and CH oscillators: an improved luminescence method for establishing solution hydration states. Journal of the Chemical Society-Perkin Transactions 2 1999, (3), 493-503.

7.   Badger, P. D. Novel Ligands for Sensitization and Protection of NIR Luminescent Lanthanide Cations. PhD Thesis, University of Pittsburgh, Pittsburgh, 2004.

8.   Dadabhoy, A.; Faulkner, S.; Sammes, P. G., Long wavelength sensitizers for europium(III) luminescence based on acridone derivatives. Journal of the Chemical Society-Perkin Transactions 2 2002, (2), 348-357.

9.   Turro, N., J., Modern Molecular Photochemistry. Sausalito, CA, 1991.

10.   Petoud, S.; Cohen, S. M.; Bunzli, J. C. G.; Raymond, K. N., Stable lanthanide luminescence agents highly emissive in aqueous solution: Multidentate 2-

hydroxyisophthalamide complexes of SM3+, Eu3+, Tb3+, Dy3+. Journal of the American Chemical Society 2003, 125, (44), 13324-13325.

11. Zhang, J.; Badger, P. D.; Geib, S. J.; Petoud, S., Sensitization of near-infrared-emitting lanthanide cations in solution by tropolonate ligands. Angewandte Chemie-International Edition 2005, 44, (17), 2508-2512.

12. Parker, D.; Senanayake, P. K.; Williams, J. A. G., Luminescent sensors for pH, pO(2), halide and hydroxide ions using phenanthridine as a photosensitiser in macrocyclic europium and terbium complexes. Journal of the Chemical Society-Perkin Transactions 2 1998, (10), 2129-2139.

13. Matthews, O. A.; Shipway, A. N.; Stoddart, J. F., Dendrimers - Branching out from curiosities into new technologies. Progress in Polymer Science 1998, 23, (1), 1-56.

14. Hawker, C., J.; Frechet, J., M., J., Preparation of Polymers with Controlled Molecular Architecture. A New Convergent Approach to Dendritic Macromolecules. J. Am. Chem. Soc. 1990, 112, 7638-7647.

15. Tomalia, D. A.; Huang, B.; Swanson, D. R.; Brothers, H. M.; Klimash, J. W., Structure control within poly(amidoamine) dendrimers: size, shape and regio-chemical mimicry of globular proteins. Tetrahedron 2003, 59, (22), 3799-3813.

16. Boas, U.; Heegaard, P. M. H., Dendrimers in drug research. Chemical Society Reviews 2004, 33, (1), 43-63.

17. Wintgens, V.; Valat, P.; Kossanyi, J.; Biczok, L.; Demeter, A.; Berces, T., Spectroscopic Properties of Aromatic Dicarboximides .1. N-H and N-Methyl-Substituted Naphthalimides. Journal of the Chemical Society-Faraday Transactions 1994, 90, (3), 411-421.

18. Klink, S. I.; Grave, L.; Reinhoudt, D. N.; van Veggel, F. C. J. M.; Werts, M. H. V.; Geurts, F. A. J.; Hofstraat, J. W., A systematic study of the photophysical processes in polydentate triphenylene-functionalized Eu3+, Tb3+, Nd3+, Yb3+, and Er3+ complexes. Journal of Physical Chemistry A 2000, 104, (23), 5457-5468.

19. de Sousa, M.; Kluciar, M.; Abad, S.; Miranda, M. A.; de Castro, B.; Pischel, U., An inhibit (INH) molecular logic gate based on 1,8-naphthalimide-sensitised europium luminescence. Photochemical & Photobiological Sciences 2004, 3, (7), 639-642.

20. Alexiou, M. S. T., Vasiliki; Ghorbanian, Shohreh; Tyman, John, H.; Brown, Robert, G.; Brittain, Patric, I., The UV-Visible Absorpyion and Fluorescence of some Substituted 1,8-Naphthalimides and Naphthalic Anhydrides. J.Chem.Soc. Perkin Trans. 1990, 2, 837-842.

21. Meech, S., R.; Phillips, D., Photophysics of Some Common Fluorescence Standards. Journal of Photochemistry 1983, 23, 193-217.

22. Haas, Y.; Stein, G., J., Pathways of Radiative and Radiationless Transitions in Europium (III) Solutions: the Role of High Energy Vibrations. J. Phys. Chem. 1971, 75, 3668.

23. Wu, C.; Brechbiel, M. W.; Kozak, R., W.; Gansow, O., A., Metal-Chelate-Dendrimer-Antibody Constructs for use in Radioimmunotherapy and Imaging. Biorg. Med. Chem. Lett. 1994, 4, 449.

24. Stolik, S.; Delgado, J. A.; Perez, A.; Anasagasti, L., Measurement of the penetration depths of red and near infrared light in human "ex vivo" tissues. Journal of Photochemistry and Photobiology B-Biology 2000, 57, (2-3), 90-93.

25. Cross, J. P.; Lauz, M.; Badger, P. D.; Petoud, S., Polymetallic lanthanide complexes with PAMAM-naphthalimide dendritic ligands: Luminescent lanthanide complexes formed in solution. Journal of the American Chemical Society 2004, 126, (50), 16278-16279.

26. Shannon, R., D., Revised effective ionic radii and systematic studies of interatomic distances in halides and chalcogenides. Acta Cryst. 1976, 32, 751-767.

27. Williams, D., H.; Fleming, Ian, Spectroscopic methods in organic chemistry. 5th. ed.; The McGraw-Hill Companies: London, 1995.

28. Wayne, C., E.; Wayne, R., P., Photochemistry. Oxford University Press: New York, 2004; Vol. 39.

29. Mecke, A.; Lee, D. K.; Ramamoorthy, A.; Orr, B. G.; Holl, M. M. B., Synthetic and natural polycationic polymer nanoparticles interact selectively with fluid-phase domains of DMPC lipid bilayers. Langmuir 2005, 21, (19), 8588-8590.